Sede Amministrativa: Università degli Studi di Padova

Dipartimento di Scienze Biomediche

DOTTORATO DI RICERCA IN SCIENZE BIOMEDICHE SPERIMENTALI

XXXI CICLO

THE ROLE OF HISTOLOGY IN THE STUDY OF TUMOR CELL METABOLISM: THE TRAP1 PARADIGM

Coordinatore: Ch.mo Prof. Paolo Bernardi

Supervisore: Dr. Andrea Rasola

Co-Supervisore: Ch.mo Prof. Paolo Bernardi

Dottorando: Marco Pizzi

To my patients

INDEX

A<small>BSTRACT</small>

Background. Metabolic reprogramming is a key feature of neoplastic transformation and mitochondria are the most important organelles in such oncogenic process. Recent evidence suggests that TRAP1 is a key player in tumor-related metabolic rewiring. Most studies have addressed TRAP1-related oncogenesis by *in vitro* and *in vivo* analyses. Little is however known on the possible contribution of histology to such studies.

Study aims. This study assessed the role of histology in the study of TRAP1-related metabolic reprogramming. Specifically, it aimed: (i) to integrate the results of *in vitro* and *in vivo* studies with the histological analysis of tumor samples; (ii) to verify the correspondence between primary human neoplasms and animal tumor models; (iv) to identify novel fields for the study of TRAP1-related oncogenic cascades.

Materials and methods. This project considered the following neoplastic settings: (i) neurofibromatosis type 1 (NF1)-related benign and malignant nerve sheath tumors; and (ii) germinal center (GC)-derived lymphoproliferative disorders. For the NF1-related tumors, morphological analysis and phenotypic characterization (TRAP1, HIF1α and related metabolic markers) were performed on: (i) human samples of plexiform neurofibroma (PN) and malignant nerve sheath tumors (MPNST); (ii) engineered mouse models of NF1-related neoplasms; and (iii) xenografts of MPNST. For GC-derived lymphomas, TRAP1 expression was assessed in non-neoplastic lymphoid tissues and in Burkitt lymphoma (BL), diffuse large B-cell lymphoma (DLBCL) and Hodgkin lymphoma (HL) samples. The immunohistochemical results were integrated with the results of *in silico* gene expression studies (Oncomine database).

Results. Histological analysis of human PNs and MPNSTs documented the expression of TRAP1, HIF1α and downstream metabolic markers in both benign and malignant samples. A progressive

increase in the positivity for such proteins was noted along the oncogenic cascade from non-neoplastic nerves to benign (PN) and malignant (MPNST) tumors. Similar expression patterns were observed in the animal tumor models. In this context, histological evaluation also proved instrumental: (i) to confirm the correspondence between human and animal tumors; (ii) to investigate the metastatic potential of MPNST xenografts; (iii) to detect the effects of *TRAP1* knock-down on tumor cell growth and metabolic reprograming; and (iv) to highlight strongly *versus* minimally activated metabolic pathways in NF1-related oncogenic cascades.

The histological characterization of reactive lymphoid tissues highlighted TRAP1 expression in subsets of GC blasts (*i.e.* differentiating immunoblasts and re-cycling centroblasts). The joint expression of TRAP1 and HIF1α in GC blasts confirmed the presence and activation of the TRAP1/HIF1α axis in GC physiology. *In silico* studies of GC-derived lymphomas showed very high *TRAP1* mRNA levels in BL and (to a lesser extent) DLBCL and HL. Immunohistochemical analysis of primary tumor samples confirmed the *in silico* results.

Conclusions. Histological analysis contributes to the understanding of tumor metabolism and integrates the results of *in vitro* and *in vivo* biochemical studies. In particular, it confirms the relevance of TRAP1 activation in NF1-related peripheral nerve sheath tumors and discloses a tight correspondence between primary human samples and animal tumor models. Immunohistochemical characterization of reactive lymphoid tissues and primary lymphoma samples also identifies specific TRAP1 expression profiles, possibly subtending tumor-related metabolic networks.

1. INTRODUCTION

Cancer cell biology relies on integrated molecular circuits, derived from the reprogramming of normal biochemical and signaling pathways. The number and kind of such derangements subtends a huge variety of neoplastic phenotypes and provides an explanation to the clinical and biological variability of human tumors. In order to maintain their growth and survival, cancer cells must nonetheless obey some general rules, broadly classifiable as (i) cancer enabling conditions and (ii) hallmarks of cancer (1). Hallmarks of cancer are acquired functional capabilities that allow cancer cell survival, proliferation and/or dissemination. These functions are made possible by general biological characteristics (*i.e.* cancer enabling conditions), which distinguish cancer cells from their non-neoplastic counterpart (1).

1.1. Cancer enabling conditions and hallmarks of cancer

According to Hanahan and Weinberg, cancer enabling conditions include (i) the genomic instability of tumor cells and (ii) the inflammatory state of premalignant and frankly malignant lesions (1).

Genomic instability is a key requisite for tumor cell biology. It mainly results from DNA changes, leading to the generation of mutant phenotypes with increased survival capacity (2). Genomic instability results from increased sensitivity to mutagenic agents and/or defects of the DNA-maintenance machinery, which physiologically detects DNA damage, activates DNA repair and neutralizes mutagenic molecules (3). Genomic instability may also derive from altered surveillance systems of cell senescence/apoptosis and from derangements of telomeric DNA. In particular, the progressive shortening of telomeres leads to chromosomal end-to-end fusions and to unstable dicentric chromosomes. This, in turn, prompts the acquisition of tumor-promoting mutations that are subsequently fixed by telomerase re-activation (4).

The presence of tumor-favoring inflammatory infiltrates is another general requisite for neoplastic transformation, as recently demonstrated in both solid and hematological tumors (5, 6). Key protagonists of such tumor-microenvironment cross-talk are specific T lymphocytes (regulatory T-cells) and accessory cell subsets (tumor-associated macrophages) (7). These cells dampen anti-tumor immune responses, favoring the ensuing of an immune-suppressive *milieu* that enables neoplastic cell survival and proliferation. Neoplastic clones, in turn, produce chemokines and cytokines that re-shape the tumor inflammatory microenvironment and indirectly promote tumor growth and dissemination (8, 9).

Besides cancer enabling conditions, tumor cells are characterized by recurrent molecular, biochemical and metabolic derangements that have been summed-up into eight major "hallmarks of cancer". These include: (i) sustained proliferative capacity; (ii) evasion form growth suppression; (iii) resistance to cell death triggers; (iv) acquisition of replicative immortality; (v) promotion of angiogenesis; (vi) acquisition of a metastasizing phenotype; (vii) evasion of anti-tumor immune responses; and (viii) reprogramming of energy metabolism (1).

The sustained proliferative capacity of tumor cells may result from either autocrine/paracrine stimulation (*i.e.* growth factors produced by the neoplastic cell themselves or by the tumor microenvironment), constitutive activation of growth factor-related signaling pathways (*e.g.* amplification or activating mutations of receptors and downstream mediators) and/or disruption of negative feedback loops (*e.g.* inactivating mutations of protein phosphatase or GTPase activity) (10).

Evasion from growth-suppressing signals largely derives from inactivating mutations in tumor suppressors genes (*e.g.* Rb and p53) (11) or in proteins involved in cell-to-cell contact inhibition (*e.g.* Merlin or LKB1) (12).

Resistance to cell death triggers and evasion from apoptosis may results from several mechanisms, including: (i) the up-regulation anti-apoptotic genes (*e.g.* over-expression of Bcl2 and related proteins); (ii) the down-regulation of tumor suppressors and DNA-damage sensors (*e.g.* loss of p53); (iii) the down-modulation of apoptotic inducers (*e.g.* Bax and Bak); and (iv) the reduced

sensitivity to extrinsic ligand-inducing death pathways (13). Recent evidence also suggests an oncogenic role for deranged autophagy, which may operate independently of or in concert with apoptosis evasion (14, 15).

The acquisition of replicative immortality is largely mediated by telomerase re-activation, which enables the progressive elongation of chromosomal ends and the avoidance of cell senescence and apoptosis (16). Recent evidence also suggests additional (telomere-unrelated) oncogenic roles for telomerase, including the amplification of Wnt signaling, the enhancement of cell proliferation and apoptosis resistance and the involvement in DNA-damage repair and RNA-dependent RNA-polymerase function (17, 18). Of note, specific tumor histotypes (*e.g.* low grade gliomas or pancreatic neuroendocrine tumors) also rely on telomerase-independent telomere maintenance, which involve recurrent mutations in the chromatin modifiers *ATRX* and *DAXX* (19).

Three further hallmarks of cancer highlight the importance of the non-tumor microenvironment, which indeed contributes to neoplastic growth by providing blood supply and pro-survival/metastasizing signals. These include induction of angiogenesis, activating invasion and metastasis and reprogramming tumor cell metabolism.

Tumor cells secrete a number of angiogenic mediators (*e.g.* VEGF, FGF) that propel the development of a rich network of aberrant vessels and contribute to oxygen and nutrient delivery, tumor cell migration and pro-tumorigenic immune cell recruitment. Angiogenesis is induced early during neoplastic transformation and is partially accomplished by the endothelial trans-differentiation of tumor cells (20) and/or by the recruitment of bone marrow-derived vascular progenitors (21).

Neoplastic cell invasion and dissemination is sustained by both cell-intrinsic molecular pathways and cell-extrinsic stromal components (*e.g.* tumor-associated macrophages, regulatory T-cells and mesenchymal stem cells). The latter further illustrate the importance of a tumor-permissive inflammatory *milieu* in order to acquire a fully-blown neoplastic phenotype (8, 9).

All of such acquired oncogenic functions require a consensus reprogramming of the metabolic features, enabling neoplastic cells to face challenging biochemical and environmental conditions. This justifies the inclusion of reprogramming energy metabolism within the hallmarks of cancer (1).

1.2 Metabolic derangements in neoplastic cells

Tumor-associated metabolic reprogramming include: (i) an increased uptake of nutrients from the extra-cellular compartment; (ii) the modulation of intra-cellular anabolic and catabolic pathways; (iii) changes in the long-range effects of cell metabolism on gene expression and micro-environmental shaping (22).

Glucose and glutamine are the principal nutrients for (neoplastic and non-neoplastic) mammalian cells. They indeed provide carbon intermediates for several biosynthetic pathways and reducing power (*i.e.* NADH, NADPH and FADH$_2$) to fuel ATP synthesis (22). Glutamine is also a source of nitrogen for the biosynthesis of nucleotides, glucosamines and non-essential amino acids and proves crucial for the uptake of essential amino acids from the extracellular space (22, 23). The key roles of glucose and glutamine prompt tumor cells to develop strategies increasing the uptake of such nutrients from the extracellular space. These include (i) the up-regulation of surface transporters for glucose (*e.g.* GLUT1) and glutamine (*e.g.* ASCT2 and SN2) (24, 25); (ii) the activation of intra-cellular enzymes blocking the efflux of glucose and glutamine back into the extra-cellular space (*e.g.* HK and phosphofructokinase for glucose; glutaminase for glutamine) (26, 27); (iii) the development of opportunistic modes for nutrient acquisition (*i.e.* macropinocytosis of extra-cellular molecules; entosis and phagocytosis of apoptotic cellular corpses) (28, 29); and (iv) the activation of self-catabolic processes (*e.g.* macro-autophagy) upon long periods of nutrient deprivation (30).

Besides nutrient uptake, tumor cells often undergo profound changes in intra-cellular metabolic pathways that propel biosynthetic reactions, while decreasing canonical catabolic circuits. This is well exemplified by the metabolic rewiring of glucose metabolism, whereby an increase in the glycolytic pathway is paralleled by a reduction of the tricarboxylic acid (TCA) cycle and oxidative
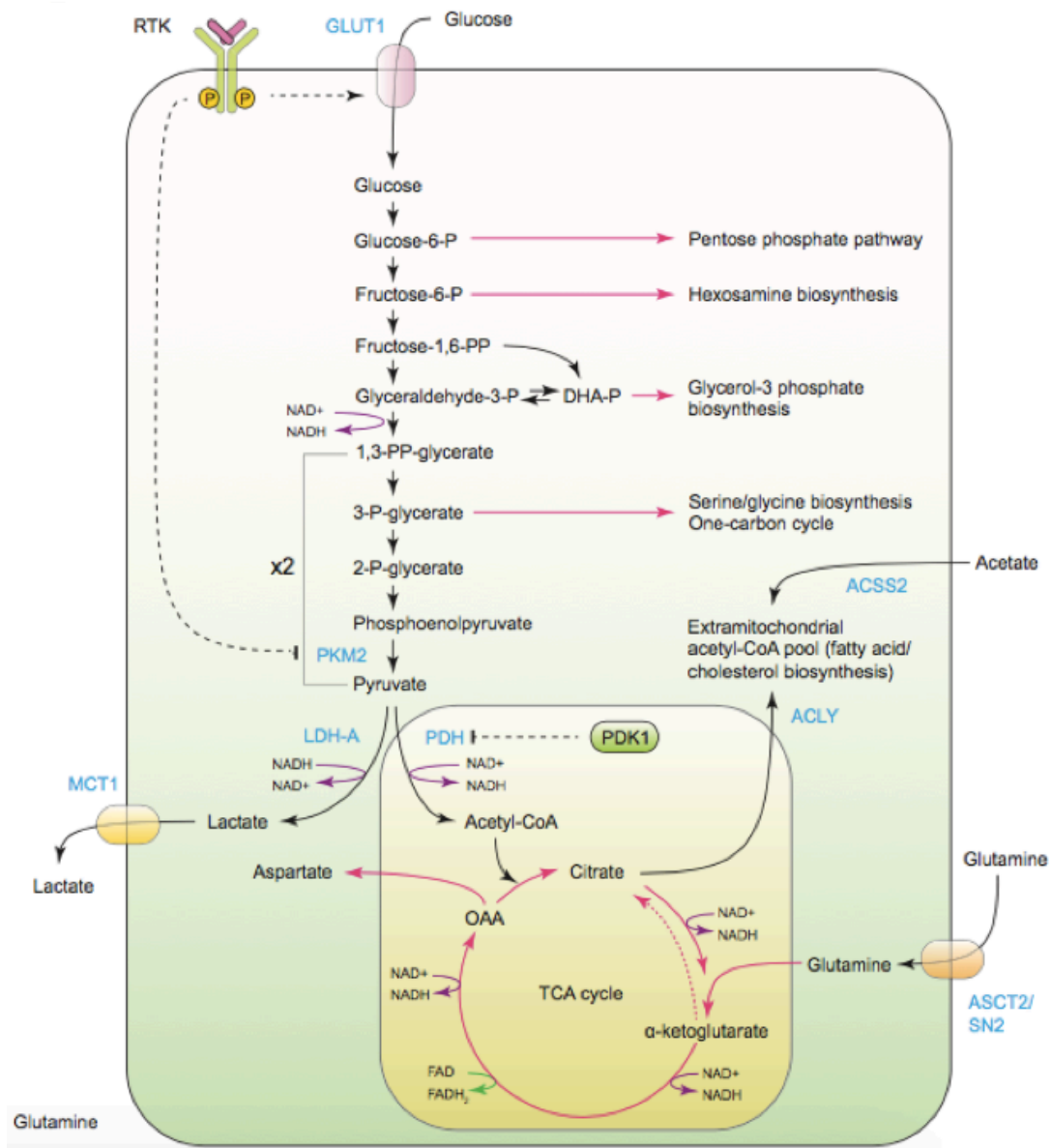
Figure 1. Biosynthetic outputs of central carbon metabolism (adapted from ref. 24)**.**
In cancer cells, the increased glycolytic flow leads to the accumulation of metabolic intermediates that may be used by several biosynthetic pathways (*i.e.* pentose phosphate pathway, phospholipid and amino acid biosynthesis). TCA cycle intermediates may also be diverted to key anabolic reactions (*e.g.* fatty acid, cholesterol and amino acid biosynthesis).

phosphorylation independently of oxygen availability (aerobic glycolysis or "Warburg effect") (31).

In such a context, the increased concentration of glycolytic intermediates can be diverted into branching pathways, generating several biosynthetic precursors (Figure 1). Glucose 6-phosphate (the first intermediate of glycolysis) can indeed enter the pentose phosphate pathway to generate ribose-5-phosphate, a structural component of nucleotides (22). Fructose-6-phosphate (the second

intermediate of glycolysis) can be diverted to hexosamine biosynthesis, thus taking part to glycosylation reactions and heparan sulfate or hyaluronic acid biosynthesis (32). Dihydroxyacetone phosphate (a derivate of Fructose-1,6-bisphosphate) can be converted into glycerol-3-phosphate and participates to the synthesis of diverse phospholipids, while 3-phosphoglycerate is a non-essential amino acid precursor and can generate methyl donor groups and reducing power (NADPH) (22, 33). In a similar way, TCA intermediates can be diverted into the synthesis of fatty acids (*i.e.* citrate conversion to acetil-CoA by ATP-citrate lyase) (34) or non-essential amino acids (*e.g.* oxaloacetate conversion to asparagine and aspartate) (35). These anabolic shifts have to be counterbalanced with an anaplerotic influx into the TCA cycle, which is mainly sustained by glutamine (36). The latter can indeed be captured within mitochondria by glutaminase, and the resulting glutamate can be converted into the TCA intermediate α-ketoglutarate by a variety of enzymes (*i.e.* glutamate dehydrogenase or amino acid transaminases) (36). Many of such metabolic derangements are promoted by oncogenes, such as HIF1 (increase of glycolytic intermediates through the inhibition of pyruvate conversion to Acetyl-CoA) (37), Akt (induction of ATP-cytrate lyases for the biosynthesis of fatty acids) (34) and c-Myc (increase of glycolytic intermediates; promotion of glutamine to glutamate conversion) (25, 38).

Finally, the metabolic reprogramming of cancer cells can induce non-metabolic derangements affecting both gene expression profiles and the tumor-microenvironment interaction. Gene expression changes are mainly caused by metabolite-induced histone modifications (*e.g.* acetylation through acetyl-CoA; crotonylation through the tryptophan and lysine derivate crotonyl-CoA; methylation through the serine derivate S-adenosyl-methionine) (39-41) or by metabolite-driven regulation of chromatin modifier enzymes (e.g. α-ketoglutarate-dependent activation of the TET2 family of DNA demethylase) (22). The tumor microenvironment can instead be influenced by the accumulation of metabolic byproducts (*e.g.* lactate) or by the active modification of the extra-cellular *milieu*. Extra-cellular lactate generates an immune permissive microenvironment (*i.e.* inhibition of dendritic cells

and T-cell activation; recruitment of tumor-favoring macrophage sub-populations), promotes angiogenesis and supports tumor invasion and metastasis (*i.e.* production of hyaluronic acid by fibroblasts; activation of matrix-degrading metalloproteinases) (42-44). Some tumors also actively modify the extra-cellular space to promote immune escape. This is the case of tryptophan degradation by tumor-derived dioxygenases (IDO1 or TDO2), which triggers amino acid deprivation-associated apoptosis of effector T-cells. A byproduct of such reactions (kynurenine) also promotes the recruitment of tumor-supporting regulatory T-cells (45).

Taken together, these data highlight the key role of metabolic reprogramming in tumor cell growth and survival. Despite most of such derangements are mediated by well-known oncogenes and transcription factors, recent studies have pinpointed the existence of novel (and only partially characterized) metabolic regulators. One of such proteins is the chaperone TRAP1.

1.3 The role of TRAP1 in tumor cell biology

TRAP1 is a 75kDa chaperone, belonging to the HSP90 family of proteins. Several lines of evidence suggest a key role for TRAP1 in the metabolic reprogramming of tumor cells (46). These functions are largely mediated by unique structural and functional features, which make TRAP1 a master regulator of mitochondrial respiration and HIF1-mediated transcriptional programs.

1.3.1   TRAP1 structure and physiological functions

TRAP1 is an ATP-binding homodimeric protein, characterized by 60% homology with HSP90. Its protomers consist of three major domains: the N-terminal domain (responsible for ATP binding and hydrolysis), the C-terminal domain (providing a dimerization site), and the middle domain (completing the ATP-binding pocket and hosting the client recognition surface). Notably, TRAP1 is the only HSP90-family member containing a N-terminal mitochondrial import sequence, which leads to its selective localization to the mitochondrial matrix (47).

TRAP1 function relies on a well-characterized cycle of structural states, leading to ATP

hydrolysis and to client protein remodeling. In detail, three conformational states have been described, including: (i) an open conformation (*i.e.* the *apo* state); (ii) a closed conformation, with a N-terminal extension between the protomers; and (iii) an intermediate conformation, with the N-terminal domains in close proximity (48). Upon binding of two ATP molecules, TRAP1 adopts a closed asymmetric conformation. This induces the first ATP hydrolysis, with subsequent structural changes and client remodeling. The second ATP hydrolysis confers a compact conformation to the protein, which induces the release of both the client and the two ADP molecules (49-51).

Several lines of evidence suggest pleiotropic functions for TRAP1, which are at least partially context- and cell-dependent. Many studies have indeed demonstrated a role for TRAP1 in the regulation of intra-cellular ROS levels and in cellular responses to oxidative stress (52, 53). In particular, TRAP1 may inhibit apoptosis by antagonizing the opening of the mitochondrial permeability transition pore (PTP). This effect can be mediated by the direct inhibition of cyclophilin D (a PTP-inducer) (54, 55) or by a reduction of ROS production from the complex II of the respiratory chain (also known as succinate dehydrogenase) (56). In a different biological context (*i.e.* regenerating liver after hepatectomy), TRAP1 has been associated with promotion of hepatic growth, modulation of intra-hepatic inflammation and tuning of fatty acid metabolism (57). Many of such functions are likely related to TRAP1 pivotal regulation of mitochondrial metabolism.

TRAP1 levels and functions are regulated at both a transcriptional and post-translational level. The latter mechanism mainly includes the phosphorylation of specific residues, which either increases its anti-oxidant functions (*e.g.* PINK1-mediated Ser/Thr phosphorylation) or finely tunes its regulation of the respiratory chain (*e.g.* c-Src and ERK1/2-mediated phosphorylation) (46, 58, 59). While the oncogenic relevance of PINK1-mediated TRAP1 regulation is largely unknown, recent evidence suggests a key role for ERK1/2-mediated TRAP1 activation in the metabolic reprogramming of tumor cells (46). This justifies the observation of high TRAP1 expression levels in several tumor histotypes (57, 60) and the positive correlation between TRAP1 levels, tumor progression and metastatic potential (27, 61-63).

1.3.2   **TRAP1 as a key player in tumor cell metabolism**

TRAP1 plays a key role in the metabolic reprogramming of tumor cells by contributing to the acquisition of an aerobic glycolytic phenotype (*i.e.* increased glycolytic activity with decreased TCA cycle and OXPHOS reactions) (57). This is largely mediated by its interaction with the complex II and complex IV of the respiratory chain. In detail, TRAP1 down-regulation of complex IV (*i.e.* cytochrome oxidase) inhibits mitochondrial respiration and promotes the accumulation of acetyl-CoA and TCA cycle intermediates, which can be used in key anabolic pathways (*i.e.* synthesis of free fatty acids and/or non-essential amino acids) (59, 64, 65). TRAP1 inhibition of complex II (*i.e.* succinate dehydrogenase) instead leads to an increase of intra-cellular succinate levels, with subsequent inhibition of prolyl-hydroxylase (PHD) and stabilization of HIF1α (a PHD target) (64). This promotes the over-expression of genes involved in glucose metabolism (*e.g.* hexokinase 2 [HK2], pyruvate kinase M2 [PKM2], glucose transporters [GLUT1, GLUT3]), cell growth (*e.g.* Cyclin F2, TGFα, TGF-β), neo-angiogenesis (*e.g.* VEFG and its receptor) and stromal invasion (*e.g.* metalloproteinase 2, c-MET, fibronectin 1) (66). These metabolic derangements, together with its anti-apoptotic (54, 56) and proteostatic functions (67), make TRAP1 a key player in human oncogenic cascades.

1.4 Paradigms of human hematological and non-hematological tumors

The study of tumor metabolism is potentially hampered by the biological heterogeneity of human neoplasms (1). Similar mediators and signaling cascades can indeed exert opposite roles in different biological and micro-environmental contexts (68). The study of tumor metabolism thus requires the identification of representative models to be assumed as paradigms of human cancer. For their well-characterized pathobiological mechanisms and non-neoplastic counterparts, neurofibromatosis type 1 (NF1)-related peripheral nerve sheath tumors and germinal center (GC)-derived peripheral B-cell lymphomas are good examples of such models.

1.4.1 Neurofibromatosis Type 1 (NF1) and NF1-associated peripheral nerve sheath tumors

Neurofibromatosis type 1 is a genetic syndrome, first described by Friederich von Rechlinghausen in 1882. It is one of the most common familial tumor predisposition syndrome with an estimated incidence of 1 in 3000 newborns. NF1 is an autosomal dominant disease with high penetrance, caused by mutations of the *Nf1* gene on chromosome 17q11.2. Almost half of cases occur *de novo* (*i.e.* NF1 with no familial history), as a result of newly acquired *Nf1* mutations during parental oogenesis or spermatogenesis.

The *Nf1* gene encodes neurofibromin, a 220-to-250 KDa GTPase-activating protein that negatively regulates the MAPK pathway by promoting Ras-bound GTP hydrolysis. As such, inactivating *Nf1* mutations lead to the constitutive activation of the MPAK pathway and promote uncontrolled cell proliferation and tumor development (69).

The clinical features of NF1 are greatly variable and consensus criteria have been established to improve the disease diagnosis (70). The prototypic clinical manifestations of NF1 include: (i) multiple cutaneous and soft tissue neurofibromas; (ii) *café-au-lait* cutaneous macules and axillary/groin freckles; (iii) iris hamartomas (also known as Lisch nodules); (iv) a higher risk of central nervous system neoplasm (optic pathway pylocytic astrocytoma; diffuse grade II to grade IV gliomas); and (v) dysplastic lesions of the sphenoid bone and long bone cortex. NF1 patients are also at increased risk of developing malignant peripheral nerve sheath tumors (MPNSTs) (71). Of note, the clinical presentation is highly variable and depends on the disease expressivity. A genotype-phenotype correlation is lacking, but whole gene deletions lead to a severe phenotype (also known as "*Nf1 microdeletion syndrome*") with mental retardation, facial dysmorphism, numerous neurofibromas and higher risk of MPNST development (72, 73), whereas in the majority of cases point mutations, as well as mosaic or segmental forms, disclose more limited and indolent disease presentations.

The most common and clinically relevant NF1-related neoplasms are peripheral nerve sheath tumors (71). These include both benign (*i.e.* neurofibromas) and highly malignant (*i.e.* MPNST)

entities. Histologically, neurofibromas are sub-classified into: (i) localized cutaneous neurofibroma (CN); (ii) plexiform neurofibroma (PN); and (iii) diffuse neurofibroma (DN). While CNs frequently affect also non-NF1 patients, PN and DN are virtually exclusive of NF1. Irrespective of the specific histotype, neurofibromas consist of an ill-defined proliferation of benign-looking Schwann cells, with scant cytoplasm and wavy nuclei. Neoplastic cells disclose a fascicular to disarranged growth pattern and are embedded in a rich non-neoplastic microenvironment, consisting of mast cells, fibroblasts/myofibroblasts and scattered lymphocytes and histiocytes. The extra-cellular stroma is often myxoid and contains numerous shredded carrot-like bundles of collagen. CNs are nodular, poorly circumscribed dermal lesions, frequently entrapping skin adnexa and nerve fibers. DNs are plaque-like dermal-hypodermal tumors, diffusely infiltrating the connective tissue and frequently displaying rounded aggregated of fibrillary material, reminiscent of tactile bodies ("Meissner-like corpuscles") (74). CNs and DNs have minimal (if any) potential of malignant transformation (75).

PNs are NF1-defining peripheral nerve sheath tumors, typically arising in the limbs, trunk and paraspinal region. They consist of multiple, variably oriented nerve fascicles that are expanded by a disorganized proliferation of Schwann cells with loose stroma. The connective tissue between the abnormal nerves is frequently occupied by a neurofibromatous proliferation closely resembling DNs. Unlike CN and DN, PN can undergo malignant transformation to MPNST (74). The molecular genetics of neurofibroma has mostly been studied in the setting of NF1. In these cases, the neoplastic transformation of Schwann cells is likely the results of the bi-allelic inactivation of the *Nf1* gene (*i.e.* germline mutation in one allele, followed by a somatically-acquired mutation in the second allele) (76). Anecdotal evidence supports the notion that sporadic neurofibromas have similar pathogenesis (*i.e.* somatic inactivation of both *Nf1* alleles) (77).

MPNSTs are aggressive soft tissue tumors disclosing neuro-ectodermal differentiation, putatively originating from the neoplastic transformation of peripheral nerve sheath-constituting cells. MPNSTs typically arise in the proximal limbs and paraspinal regions. In many cases, a

direct connection/close contiguity with major nerves (*e.g.* the sciatic nerve) and/or nerve roots is documented. MPNSTs occur either sporadically or in NF1 patients. In the latter case, the lifetime risk of developing MPNST is estimated between 2% and 10% (78). MPNSTs present as large, often necrotic and hemorrhagic masses. Low grade lesions may however simulate PNs or less aggressive sarcoma types. Histologically, MPNSTs are characterized by a variety of cytology and growth patterns that often mask their peripheral nerve sheath derivation. The tumor is indeed composed by spindle to epithelioid and/or pleomorphic malignant cells, occasionally featuring heterologous differentiation toward chondrosarcomatous, osteosarcomatous and/or rhabdomyosarcomatous components. Tumor cells usually disclose a fascicular to storiform growth pattern. A rather typical finding is the alternation of hyper- and hypo-cellular areas, with dense cell aggregates around medium-sized blood vessels. Fibrosarcoma-like herringbone areas and branching hemangiopericytoma-like vessels can also be documented. Given the broad variety of morphological features, a definite diagnosis of MPNST is only made by the presence of a clear-cut peripheral nerve sheath phenotype (*e.g* at least focal immunohistochemical positivity for S100 and/or SOX10).

The molecular genetics of MPNSTs have been extensively studied. Most cases disclose a complex karyotype with structural and numerical chromosomal derangements. Recurrent monosomy of chromosome 22 and amplification of distal chromosome 17q have been documented in small subsets of cases (71). At a gene level, *Nf1* inactivation is frequently documented in both NF1-related and sporadic cases, likely representing an early oncogenic event. Recurrent imbalances also include p16 inactivation and PRC2 loss of function. The latter is a polycomb repressor complex that regulate the transcription of several Ras-dependent genes (79). In the MPNST setting, its deregulation amplifies the abnormal MAPK-related signals, deriving from *Nf1* inactivation (80). At present, nothing is known about the functional effects of such molecular derangements on tumor cell metabolism. Furthermore, no data are as yet available on the metabolic rewiring occurring along the PN to MPNST oncogenic cascade.

1.4.2 Germinal center-derived B-cell lymphoproliferative disorders

Peripheral B-cells lymphomas are a broad group of lymphoproliferative disorders, derived from the neoplastic transformation of mature B lymphocytes. The current classification of such tumors is based on their putative non-neoplastic counterpart and include entities derived from: (i) pre-germinal center (GC) B-cells (*i.e.* lymphocytes that are not antigen-primed and have not undergone GC reactions); (ii) GC B-cells (*i.e.* lymphocytes passing through the GC and up-regulating GC-related genes); and (iii) post-GC B-cells (*i.e.* lymphocytes that have passed through the GC and are committed to plasma cells or memory B cell differentiation) (81).

The majority of peripheral B-cell lymphomas derive from GC B-cells, given the complex chromosomal and genetic events that physiologically occur within this anatomic compartment. The GC is indeed the site of immunoglobulin gene somatic hyper-mutation (SHM) and class switch recombination (CSR) (82). These biological processes result from a sharp functional and anatomic compartmentalization, by which different lymphoid populations segregate into distinct GC areas. The GC consists of a dark zone (DZ) and a light zone (LZ). The former is populated by large proliferating centroblasts, with coarse chromatin and multiple peripherally-located nucleoli. The latter is populated by mature centrocytes with irregular nuclear contours and dense chromatin. In the DZ, antigen-primed B-cells over-express the transcriptional regulator *BCL6* and undergo SHM. In the LZ, the centroblasts acquire a centrocyte morphology, up-regulate *IRF4* and *BLIMP1* and undergo CSR. They can then re-enter the DZ (for a further cycle of SHM) or leave the GC to terminally differentiate into plasma cells or memory B-cells (83). The molecular bases of LZ fate decision are only partially elucidated, but recent evidence suggests a key role for *MYC* and *IRF4/BLIMP1* transcription factors (82). *MYC* expression would promote
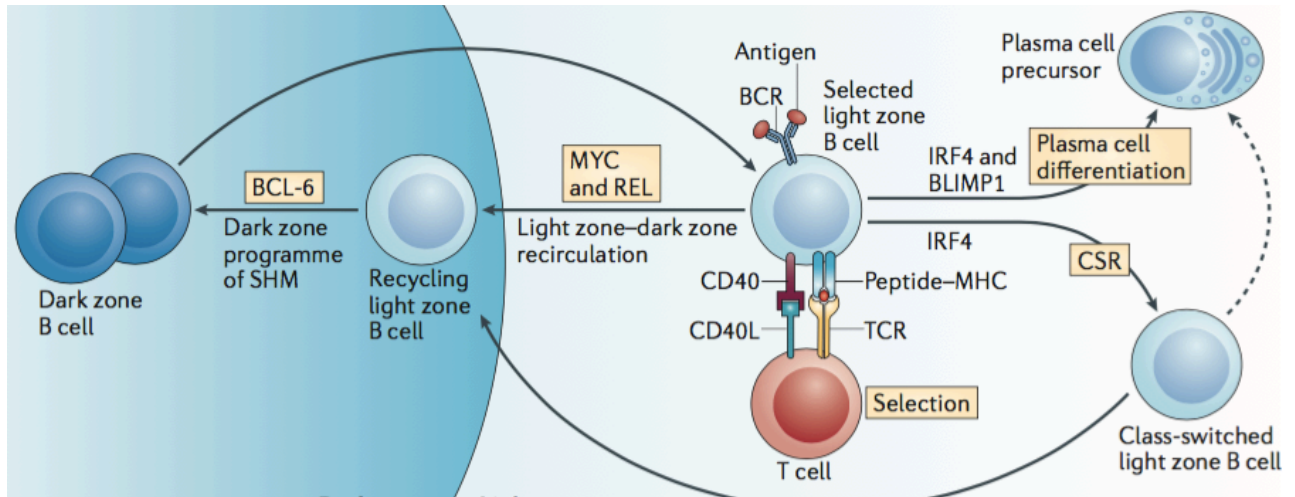
Figure 2. Molecular bases of LZ B-cell fate decision (adapted from ref. 85).
Antigen-primed LZ B-cells can either differentiate into plasma cells or re-enter the DZ for a further cycle of somatic hypermutation (SHM). Plasma cell differentiation is promoted by transcription factors such asIRF4 and BLIMP1, while DZ re-entry is prompted by c-Myc and REL expression.

_____

the re-entry of B-cells into the DZ (84), while *IRF4* and *BLIP1* inhibit *BCL6* transcription and prompt the terminal differentiation of B-cells (83, 85) (Figure 2).

This complex immunologic scenario provides a framework to the biology and clinic-pathological features of GC-derived peripheral B-cell lymphomas, which include: (i) follicular lymphoma (FL); (ii) Burkitt lymphoma (BL); (iii) a subset of diffuse large B cell lymphomas, not otherwise specified (DLBCL); and (iv) Hodgkin lymphomas (HL).

FL represents about 20% of non-Hodgkin lymphomas and affects adult to elderly patients with a clear-cut female preponderance (86). Histologically, the tumor consists of a heterogeneous population of neoplastic cells with variable proportions of mature centrocytes and proliferating centroblasts. The cells are arranged in a nodular, nodular and diffuse, or purely diffuse growth pattern (81). Based on the centroblast content, FL is graded into a three-tiered scale (G1: <5 centroblasts/10 high-power fields [HPF]; G2: 5-15 centroblasts/10 HPF; G3: >15 centroblasts/10 HPF, further sub-classified into G3A and G3B, depending on the presence or absence of residual centrocytes). The majority of cases are either G1, G2 or G3A lymphomas and disclose a relatively

indolent clinical course (87). By contrast, G3B FLs are biologically aggressive tumors, which clinically resemble DLBCL (86). Gene expression studies have highlighted a LZ origin for FLs, irrespective of the tumor grade (88).

DLBCL and BL are clinically aggressive lymphomas, composed by sheets of blasts with no evidence of mature centrocytes. DLBCLs are a heterogeneous group of tumors, accounting for about 40% of all non-Hodgkin B-cell lymphoma. They can arise *de novo* or as secondary transformation of prior low-grade neoplasms. DLBCLs are composed of large blasts with either centroblastic, immunoblastic or anaplastic morphology (81). The tumor phenotypic and molecular features are highly variable and correlate with the putative cell of origin (89). A subset of DLBCLs indeed discloses gene expression profiles and immunohistochemical features akin to GC-residing B-cells (*i.e.* GCB type DLBCL), while others have molecular and phenotypic features closer to B-cells committed to post-GC differentiation (*i.e.* ABC type DLBCL). A third group has poorly-defined molecular features and (for clinical and diagnostic purposes) is lumped together with the ABC type into a "non-GCB type" category (89, 90). Beyond the cell of origin stratification, recent studies have highlighted further DLBCL-specific transcriptional programs and more complex molecular landscapes (91-94). Little is however known on the metabolic features of these lymphomas.

BL is much rarer than DLBCL, accounting for only 1-2% of non-Hodgkin lymphomas. It frequently affects children and young adults and constitutes up to 50% of pediatric lymphoma cases. Three clinical variants are recognized: (i) endemic (*i.e.* African) BL; (ii) sporadic BL (most frequently encountered in Western countries); and (iii) immunodeficiency-related (commonly HIV-associated) BL. Histologically, the tumor is composed by medium-sized, immature-looking cells with finely-dispersed chromatin and inconspicuous nucleoli. Scattered histiocytes are frequently present within the neoplastic proliferation and confer a "starry sky" pattern to the tumor. The neoplastic cells invariably express GC-specific markers (Bcl6 and CD10) and are consistently negative (or only weakly positive) for Bcl2. BL is a highly proliferative tumor, with

a mean Ki67 index >98% (81). Cytogenetically, the tumor cells invariably disclose translocations that juxtapose the *MYC* gene on chromosome 8q24 to the immunoglobulin genes on chromosomes 14q11, 2p12 or 22q11 (95). This, in turn, leads to the oncogene constitutive over-expression and to the uncontrolled proliferation of tumor cells. Endemic and immunodeficiency-related BLs are frequently associated with EBV infection, while sporadic cases rarely feature such an association (96). Unlike FL and DLBCL, gene expression studies indicate a DZ origin for BL (88).

HLs account for about 15% of all lymphoproliferative disorders and disclose peculiar clinic-pathological and biological features. They frequently arise in adolescents and young adults, present as cervical and/or mediastinal lymphadenopathies and are histologically characterized by small numbers of neoplastic cells, embedded in a rich inflammatory microenvironment. Tumor cells are large, with mono/multi-lobated nuclei and abundant slightly eosinophilic cytoplasm (81). Based on histological and clinical features, HLs are classified in two entities: (i) classical HL (cHL) and (ii) nodular lymphocyte-predominant HL (NLPHL). cHL is characterized by both mononuclear (Hodgkin) and multinucleated (Reed-Sternberg) neoplastic cells. Hodgkin and Reed-Sternberg (HRS) cells are closely related to each other and disclose a B-cell defective phenotype, with strong positivity for CD30 (100% of cases) and CD15 (85% of cases), weak positivity for PAX5 and almost complete negativity for CD20, CD22, CD79a and CD19. According to the micro-environmental features, four variants of cHL are described (*i.e.* nodular sclerosis, mixed cellularity, lymphocyte-rich and lymphocyte-depleted variants) (97). NLPHL is characterized by slightly different neoplastic cells, referred to as LP elements. These are large blast-like cells with abundant cytoplasm, convoluted nuclei and multiple, small basophilic nucleoli. Unlike RSH, they have a full B-cell phenotype (strong positivity for PAX5, CD20, CD22, CD79a and CD19), rarely express CD30 and are invariably negative for CD15 (98). The majority of NLPHL disclose a nodular growth pattern, with LP cells residing within expanded and distorted GCs. Rare immuno-architectural variants are also described (*i.e.* serpiginous;

nodular with prominent extra-nodular LP cells; T-cell rich nodular; T-cell/histyocyte-rich large B-cell lymphoma-like; and diffuse B-cell rich pattern) (99). The molecular features and biological origin of HRS and LP cells have long been debated. Recent gene expression analysis on micro-dissected neoplastic cells have however demonstrated a GC origin for both cHL and NLPHL. In detail, LP cells may originate from GC lymphocytes of the LZ that are undergoing differentiation into memory B-cells (100). By contrast, cHL likely derive from LZ B-cells that have undergone abortive plasma cell differentiation (101, 102). Similarly to what reported for non-Hodgkin lymphomas, little is currently known on the metabolic features of both cHL and NLPHL.

2. STUDY AIMS

This study assessed the role of histology in the study of tumor cell metabolism. In particular, it aimed:

- To apply morphological, morphometric and immunohistochemical analysis to the study of TRAP1-related oncogenic cascades;

- To integrate the results of *in vitro* and *in vivo* studies with the histological assessment of tumor samples;

- To verify the correspondence between human neoplasms and tumor animal models;

- To identify novel fields for the study of TRAP1-related oncogenic cascades.

3. MATERIALS AND METHODS

3.1 Histological samples

The histological characterization of TRAP1-related oncogenic cascades was organized in two sections: (i) a non-hematological tumor branch (NF1-related peripheral nerve sheath tumors); and (ii) a hematological tumor branch (GC-derived peripheral B-cells lymphomas and Hodgkin lymphomas).

As for the non-hematological tumor branch, both primary human neoplasms and tumor animal models were analyzed. In detail, the primary human samples included: (i) 10 cases of sub-cutaneous/soft-tissue PN; (ii) 10 cases of MPNST from NF1-patients; and (iii) 5 surgical samples of major nerve trunks (non-neoplastic counterpart of both PN and MPNST). All cases were retrieved from the archives of the General Pathology and Surgical Pathology Unit, Department of Medicine-DIMED (University of Padova – Italy). The animal tumor models included: (i) 7 paired (TRAP1 wild-type and knock-down) PN samples from an engineered mouse model (see below); (ii) 5 paired (TRAP1 wild-type and knock-down) MPNST from an engineered mouse model (see below); (iii) 5 patient-derived tumor xenografts (PDTX) of MPNST (kindly provided by Dr Conxi Lazaro, Translational Research Laboratory ICO-IDIBELL, L'Hospitalet de Llobregat; Barcelona – Spain) (103); (iv) 5 tumor xenografts obtained from the sub-cutaneous injection of nude mice with immortalized cisMPNST cells (*i.e.* murine MPNST cells lacking both *Nf1* and *TP53* genes, kindly provided by Dr Le and co-workers, University of Texas Southwestern Medical Center, Dallas - TX, USA).

The hematological tumor branch considered primary lymphoma samples from patients with DLBCL (n=33), BL (n=5), cHL (n=5), and NLPHL (n=5). DLBCLs included both adult and pediatric cases, with either a GCB (n=28) or non-GCB (n=5) phenotype, according to Hans algorithm (90). Lymph node (n=5) and tonsil (n=5) samples with reactive lymphoid hyperplasia were also included (non-neoplastic counterpart of the aforementioned lymphoma entities). All adult cases were retrieved

from the archives of the General Pathology and Surgical Pathology Unit, Department of Medicine-DIMED (University of Padova – Italy). Pediatric cases were instead obtained from the national archive of the Associazione Italiana Ematologia Oncologia Pediatrica (AIEOP; Surgical Pathology Unit, San Bortolo Hospital; Vicenza – Italy). For all samples, the institutional regulations on research on human and animal tissues were followed, according to the Declaration of Helsinki.

3.2 Engineered mouse model of NF1-related PN and MPNST

Mouse models of NF1-related PN and MPNST were obtained through a collaboration with Prof. Lu Le, University of Texas Southwestern Medical Center (Dallas - TX, USA). In summary, murine nerve sheath tumors were obtained by isolating dorsal root ganglia (DRG) from E13.5 engineered mouse embryos (*i.e.* embryos carrying loxP sequences adjacent to specific target genes). The obtained cells were subsequently infected with adenovirus carrying the *Cre* recombinase. Floxed and control cells were implanted in the sciatic nerve of nude mice to develop discrete tumor masses (104). The murine model of NF1-related PN was obtained by using embryonal DRG cells carrying $Nf1^{flox/flox}$ genes (*i.e.* tumor precursors with inducible loss of the sole *Nf1* gene). Murine NF1-related MPNSTs were instead obtained by using donor embryos with both $Nf1^{flox/flox}$ and $TP53^{flox/flox}$ genes (*i.e.* tumor precursors with inducible loss of both *Nf1* and *TP53*).

To assess TRAP1 oncogenic role in NP and MPNST murine models, expression of the protein was modulated through RNA interference, as previously described (*i.e.* adenovirus-mediated transfection of either TRAP1-targeting shRNAs or scrambled shRNAs via pLKO.1 plasmids) (64).

3.3 Tissue microarray (TMA) generation

Tissue microarrays (TMA) were obtained from primary human lymphoma samples with sufficient diagnostic material, as previously reported (105). This allowed the cost-effective assessment of a large number of cases under standardized and reproducible conditions. In detail, after selection of representative tumor areas, 2 tissue cores were obtained for each donor block (core

diameter: 0.1 cm). Tissue cores were then included in a recipient block together with positive and negative controls (positive controls: reactive lymph nodes and tonsils; negative controls: hepatic and cardiac tissue). From each TMA block, 4 μm-thick tissue sections were obtained for immunohistochemical analysis. The TMA construction was performed by using the *Galileo TMA CK3500* device (Integrated System Engineering, Milan – Italy).

3.4 Morphological characterization

Each tumor sample was morphologically characterized: (i) to confirm the originally proposed diagnosis (primary human samples); (ii) to assess the correspondence between human neoplasms and tumor animal models (engineered mice and xenograft models); and (iii) to select the most representative tumor areas for immunohistochemical analysis.

Morphological evaluation was performed on 3 to 4 μm-thick tissue sections stained with standard hematoxylin and eosin (H&E). As for the solid tumor branch of the study, histological criteria for the diagnosis of PN were set as follows: (i) presence of disarranged nerve bundles with loose to myxoid stroma; (ii) detection of variable stromal and inflammatory cell types (*i.e.* neoplastic Schwann cells, fibroblasts/myofibroblasts, mast cells, lymphocytes, plasma cells and histiocytes); (iii) lack of atypical cytological features; (iv) absent or extremely low mitotic activity (<1 mitosis/10 high-power fields); and (v) lack of tumor cell necrosis (74). By contrast, histological criteria for the diagnosis of MPNST included: (i) a highly cellular proliferation of atypical mesenchymal cells, arising from (or lying in close proximity to) major nerve trunks; (ii) the paucity of non-neoplastic inflammatory and/or stromal cells; (iii) the documentation of obvious mitotic activity (>5 mitoses/10 high-power fields); and/or (v) the documentation of tumor cell necrosis (74). As for the hematological tumor branch, each entity was diagnosed according to the revised 4th edition of the WHO Classification of lymphoid tumors (81).

3.5 Immunohistochemical analysis

Immunohistochemical analysis was performed on 3 to 4 μm-thick tissue sections, stained with the following primary antibodies: anti-TRAP1 (clone sc-73604, Santa Cruz, Dallas – TX, USA), anti-HIF1α (clone NB100-449, Novus Biologicals, Littleton – CO, USA), anti-PKM2 (clone D78A4, Cell Signaling Technology, Danvers – MA, USA), anti-Nf1 (clone sc-20017, Santa Cruz, Dallas – TX, USA9), anti-GLUT1 (clone, Dako), anti-HK2 (clone sc-6521, Santa Cruz, Dallas – TX, USA), anti-Glutamine Synthetase (clone ab16802, Abcam, Cambridge - UK), anti-CD117 (polyclonal, Dako, Glostrup - Denmark), anti-PAX5 (clone 1H9; Thermo Fisher Scientific, Waltham – MA, USA), anti-cMyc (clone EP121, Epitomics, Burlingame, CA – USA), and anti-IRF4/MUM1 (clone MUM1p, Dako, Glostrup - Denmark). Antigen retrieval was performed with heat/EDTA in the Bond-Max automated immunostainer (Leica Biosystems, Milan – Italy), as previously described (105).

Immunohistochemical analysis was performed with both single (TRAP1, HIF, Nf1, GLUT1, PKM2) and double immunostaining (TRAP1/CD117, TRAP1/PAX5, TRAP1/c-Myc, TRAP1/IRF4). For single immunostaining the Bond™ Polymer Refine Detection kit (Leica Biosystem, Newcastle, UK) was used. Double immunostaining were performed using the Bond™ Polymer Refine Detection and Bond™ Polymer Refine Red Detection kits (Leica Biosystem). Histological pictures were acquired by the DFC420 digital camera and software (Leica Biosystems).

3.6 *In silico* gene expression analysis

To assess TRAP1 mRNA expression levels in non-Hodgkin B-cell lymphomas and Hodgkin lymphoma, the Oncomine database and gene microarray analysis tool was explored (August 2018; http//:www.oncomine.org) (106). Inclusion criteria for the *in silico* analysis were set as follows: (i) gene expression studies had to assess *TRAP1* mRNA levels in both BL, DLBCL, and HL (of any type); (ii) *TRAP1* expression data had to be assessed in ≥ 5 cases for each considered entity. Such inclusion criteria were met by three publicly available data sets (100, 107, 108).

3.7 Morphometric and statistical analysis

Morphometric analyses were performed through digital imaging techniques, by using the DMD108 microscope and software (Leica Microsystems, Milan - Italy). Statistical analysis was performed using non-parametric tests to compare quantitative variables (Mann-Whitney U test). Differences between groups were considered statistically significant for p-values below 0.05.

4.1 TRAP1 in NF1-related peripheral nerve sheath tumors

The histological characterization of NF1-related peripheral nerve sheath tumors was first conducted on primary human neoplasms. The obtained results were then compared with the morphological and immunohistochemical features of the animal tumor models.

4.1.1 Histological characterization of human PNs and MPNSTs

The morphological and immunohistochemical characterization of primary human samples was performed by comparing PNs and MPNSTs with their non-neoplastic counterpart (*i.e.* peripheral nerve trunks). In such samples, the whole TRAP1-related oncogenic cascade was immunohistochemically tested, moving from the assumption that *Nf1* loss would prompt MAPK hyper-activation, TRAP1-mediated stabilization of HIF1α and increased transcription of HIF1-target genes. In line with this hypothesis, both PN and MPNST disclosed consistent immunohistochemical negativity for Nf1, with strong expression of pERK and variable positivity for TRAP1, HIF1α and HIF1 targets (*i.e.* GLUT1, HK2, PKM2). Non-neoplastic nerve trunks were instead negative for both TRAP1 and its downstream targets (Figure 3A).

In detail, TRAP1 was expressed by only a subset of cells within PNs, while strong positivity was observed in all MPNSTs. In all cases, TRAP1 expression disclosed a finely granular cytoplasmic pattern, consistent with mitochondrial localization. Furthermore, double immunostain for TRAP1 and CD117 disclosed two subsets of TRAP1-expressing cells: (i) a TRAP1-positive/CD117-positive population, consistent with intra-tumor (non-neoplastic) mast cells; and (ii) a TRAP1-positive/CD117-negative population, with cytological and topographic features consistent with neoplastic Schwann cells. Similar expression patterns were observed for HIF1α, with complete negativity of non-neoplastic nerves, weak-to-moderate positivity in subsets of NP cells and diffuse

positivity in all MPNSTs. Of note, HIF1α downstream targets disclosed variable expression profiles. In particular, PNs featured partial positivity for PKM2 with nearly complete negativity for GLUT1 and HK2. By contrast, MPNSTs were characterized by higher (yet variable) GLUT1 and HK2 positivity, with strong and diffuse expression of PKM2 in most cases. Taken together, these results suggest a progressive up-regulation of the TRAP1/HIF1α axis along the MPNST oncogenic cascade (Figure 3A).

Notably, the over-expression of genes related to glucose metabolism (*i.e.* GLUT1, HK2 and PKM2) was paralleled by the up-regulation of Glutamine Synthetase (GLUL), a key enzyme for glutamine biosynthesis and metabolism. Indeed, GLUL was almost completely absent in non-neoplastic peripheral nerves, partially positive in PNs and strongly expressed in all MPNSTs (Figure 3A).

4.1.2 Histological characterization of animal tumor models

The histological characterization of animal tumor models was mainly aimed to: (i) evaluate the correspondence between primary human neoplasms and *in vivo* murine tumors; (ii) define the expression and distribution of TRAP1 and its downstream targets; (iii) assess the histological effects of TRAP1 knock-down in both PN and MPNST; and (iv) define the metastatic potential of sub-cutaneous MPNST xenografts.

As for the *in vivo* engineered mouse model, the morphological analysis of sciatic nerve tumors disclosed a perfect correspondence between human neoplasms and their putative murine counterpart. In particular, sciatic tumors arose from $Nf1^{floxed/floxed}$ DRG cells recapitulated the histological features of PN (*i.e.* haphazardly arranged nerve bundles with loose stroma, benign-looking Schwann cells and varying numbers of stromal and inflammatory cells). By contrast, $Nf1^{floxed/floxed};TP53^{floxed/floxed}$ cells gave rise to biologically aggressive neoplasms akin to MPNSTs (*i.e.* large necrotic masses composed of atypical, mitotically active neoplastic cells with little
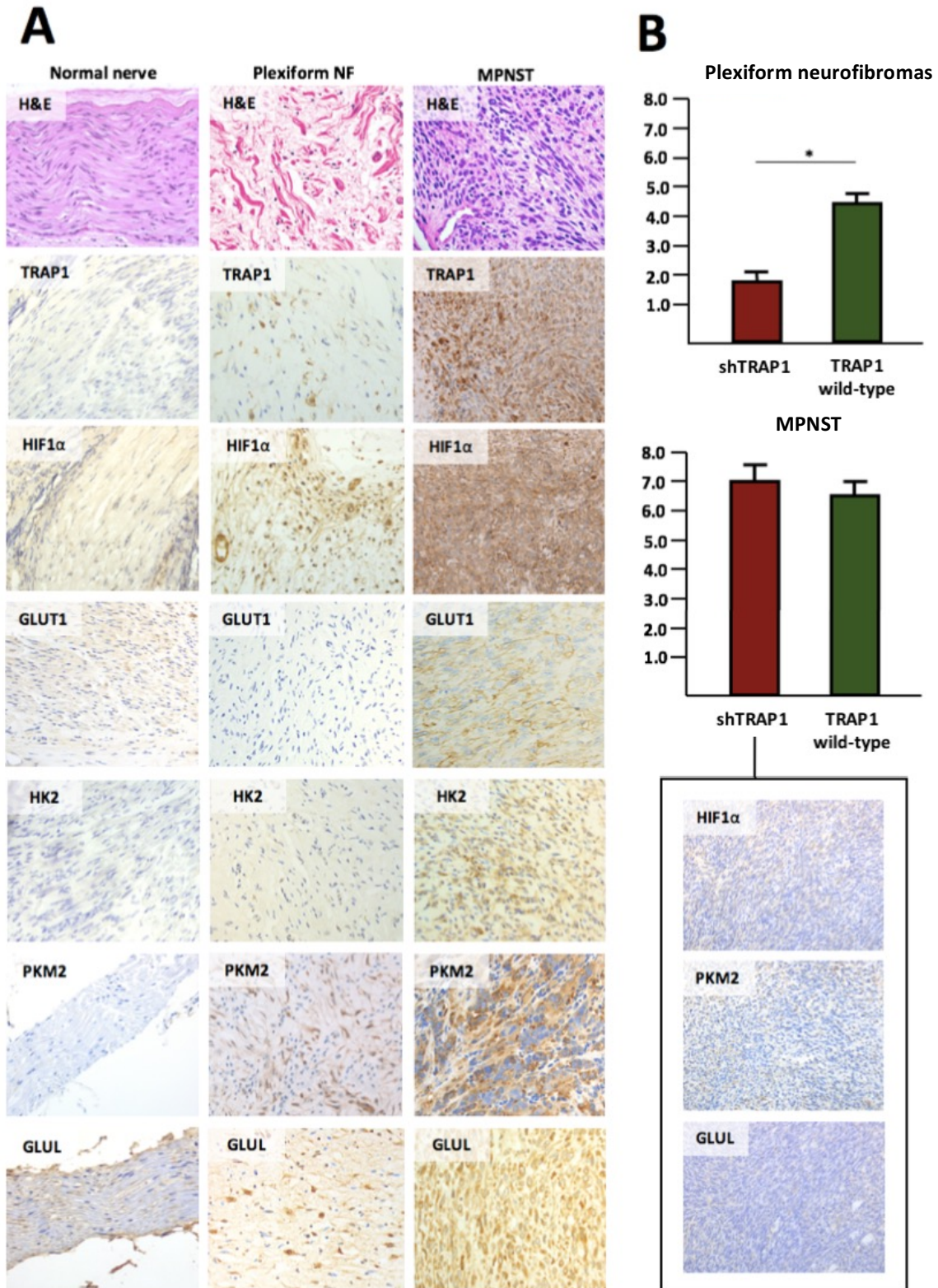
Figure 3. Histological features of NF1-related peripheral nerve sheath tumors.
A. In human samples, TRAP1, its downstream targets (GLUT1, HK2 and PKM2) and GLUL were negative in normal nerves, weakly/partially positive in PNs and highly expressed in MPNSTs. **B.** In an engineered mouse model, shTRAP1 PNs were significantly smaller than wild-type tumors (main diameter assessed in millimeters by digital imaging techniques); no significant differences in tumor diameter were instead noted between shTRAP1 and wild-type MPNSTs. In MPNST, TRAP1 silencing was nonetheless associated with the down-modulation of HIF1α, HIF1 targets and GLUL (H&E and peroxidase stains; original magnification 20x. The asterisk indicates a *p*-value <0.05).

29

intervening stroma). This murine models also allowed to evaluate the histological effects of TRAP1 silencing in NP and MPNST. In particular, TRAP1 knocked down $Nf1^{floxed/floxed}$ cells generated much smaller tumors compared to wild-type cells (mean tumor size, as histologically assessed: 0.19 cm versus 0.42 cm; p< 0.05) (Figure 3B). No statistically significant differences in tumor size were instead noted between MPNSTs with knocked-down or wild-type TRAP1 (mean tumor size: 0.70 cm *versus* 0.65 cm; p= 0.27). In such tumors, however, TRAP1 silencing was associated with decreased expression of HIF1α, HIF1-regulated genes (*i.e.* PKM2, HK2 and GLUT1) and GLUL (Figure 3B).

Immunohistochemical analysis was thoroughly applied to assess TRAP1 expression in normal murine tissues and to characterize TRAP1, HIF1α, HIF1 targets and GLUL expression along the MPNST oncogenic cascade. In non-neoplastic tissues of wild-type mice, TRAP1 expression was documented in cardiomyocytes, brown adipocytes, peri-venular hepatocytes, renal tubules and histiocytes of the splenic red pulp, with consistent negativity in peripheral nerves, skeletal muscles, blood vessels, pneumocytes, lymphocytes of the splenic red pulp and primary lymphoid follicles, colocytes and renal glomerular cells (Figure 4A-H). The immunohistochemical profile of murine PN and MPNST tumors recapitulated the one observed in human samples (*i.e.* progressive increase of TRAP1 and HIF1α expression from non-neoplastic nerves to PN and MPNST; variable positivity for HIF1 targets, with highest expression of PKM2; progressive increase in GLUL positivity).

The immunohistochemical characterization of PDTXs was in keeping with what observed in primary human samples and *in vivo* engineered MPNSTs. By contrast, xenografts of the immortalized cysMPNST cell line were characterized by slightly different expression profiles (weaker HIF1α, HK2 and GLUL compared to primary human samples). This latter model proved instrumental also to characterize the metastatic potential (and overall biological aggressiveness) of sub-cutaneous tumor xenografts. In particular, autopsy and histological examination at the end of the experiment (18 days after sub-cutaneous injection of 10^6 cysMPNST cells) did not show any evidence of disseminated disease in the brain, lungs, liver, spleen, kidneys, bone marrow, heart and/or skeletal muscle. Taken
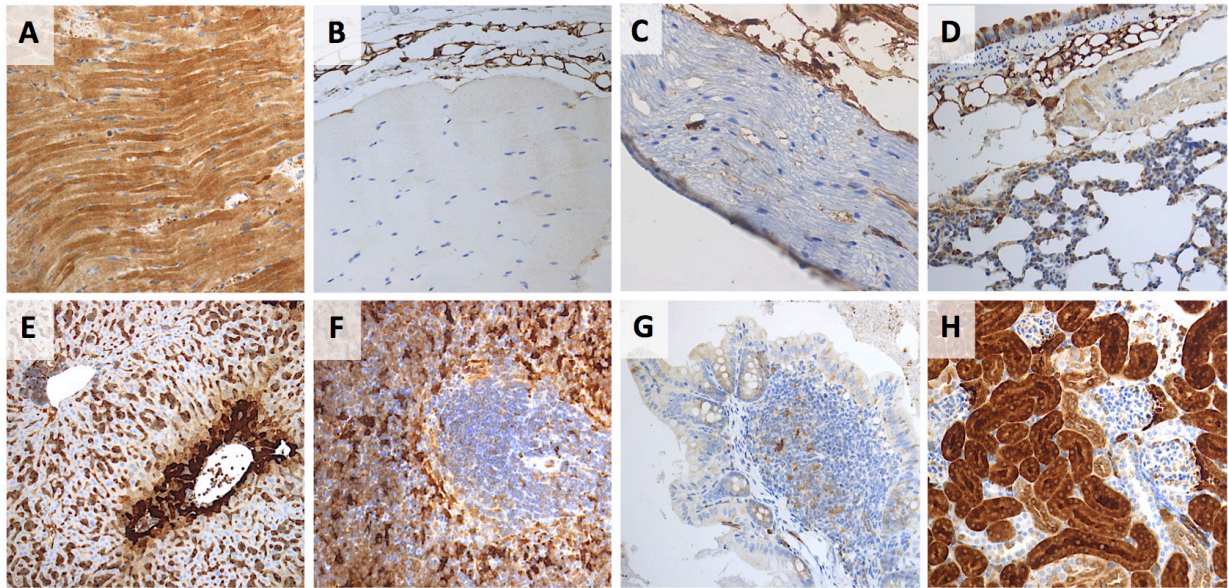
Figure 4. TRAP1 expression in non-neoplastic murine tissues.
In wild-type mice, TRAP1 was diffusely expressed in the heart (**A**), brown fat (**B**, **C** and **D**, *top panel*), peri-venular hepatocytes (**E**), splenic red pulp histiocytes (**F**) and renal tubular cells (**H**). Consistent negativity was instead observed in skeletal muscles (**B**, *lower panel*), peripheral nerves (**C**, *mid to lower panel*), pneumocytes and blood vessels (**D**, *top to lower panel*), splenic white pulp (**F**), colonic epithelial cells and lymphoid follicles (**G**) and renal glomeruli (**H**). (Peroxidase stains; original magnification 10x and 20x).

together, these results suggest slightly different metabolic features and reduced biological aggressiveness for subcutaneous xenograft of immortalized MPNST cells.

4.2 TRAP1 in non-neoplastic and neoplastic lymphoid cells

Most studies addressing TRAP1-related oncogenesis have focused on solid tumor models. Little is instead known on TRAP1 expression in non-neoplastic and neoplastic lymphoid cells. To fill this gap, the hematologic tumor branch of the present study first assessed TRAP1 expression in a series of non-neoplastic (*i.e.* reactive) lymph nodes and tonsils. The obtained results prompted the immunohistochemical characterization of selected lymphoma entities.

4.2.1 TRAP1 expression in non-neoplastic lymphoid cells

TRAP1 immunostaining on reactive lymph nodes and tonsils disclosed a clear-cut positivity in a minority (10% to 40%) of GC cells. In detail, strong cytoplasmic staining was observed in both GC-residing macrophages (also known as "tangible body cells") and in subsets of DZ and LZ large lymphoid blasts (Figure 5A-B). Mature-looking GC centrocytes and inter-follicular lymphocytes were consistently TRAP1-negative.

To elucidate the nature of the TRAP1-positive GC blasts, double immunostainings were performed on whole tissue sections. The joint assessment of TRAP1 and PAX5 (a pan-B cell marker) disclosed a B-cell origin for all TRAP1-positive GC blasts (Figure 5C). Furthermore, TRAP1/IRF4 double immunostainings showed three populations of cells: (i) a TRAP1-positive/IRF4-positive population of large blasts, likely representing LZ B-cells skewed toward plasma cell differentiation; (ii) a TRAP1-positive/IRF4-negative blast population, possibly representing a DZ-recycling blast pool; and (iii) a TRAP1-negative/IRF4-positive population of small-to-medium sized differentiated plasma cells and plasmacytoid lymphocytes (Figure 5D). TRAP1 expression in DZ-recycling blasts was further confirmed by TRAP1/c-Myc double immunostaining, which indeed showed the joint expression of the two markers in a consistent subset of GC B-blasts (Figure 5E). Finally, immunohistochemical analysis disclosed HIF1α expression in a sub-set of GC B-cells consistent with the TRAP1-positive population. These overall results highlight TRAP1 expression in specific subsets of GC B-cells and suggest a possible role of the TRAP1/HIF1α axis in GC-based immune responses.

4.2.2 TRAP1 expression in GC-derived lymphoproliferative disorders

The results on non-neoplastic GC B-cells led to assess TRAP1 expression in the putative neoplastic counterparts of such elements (*i.e.* GC-derived B-cell non-Hodgkin and Hodgkin lymphomas). This analysis was conducted at a both mRNA and protein expression level.
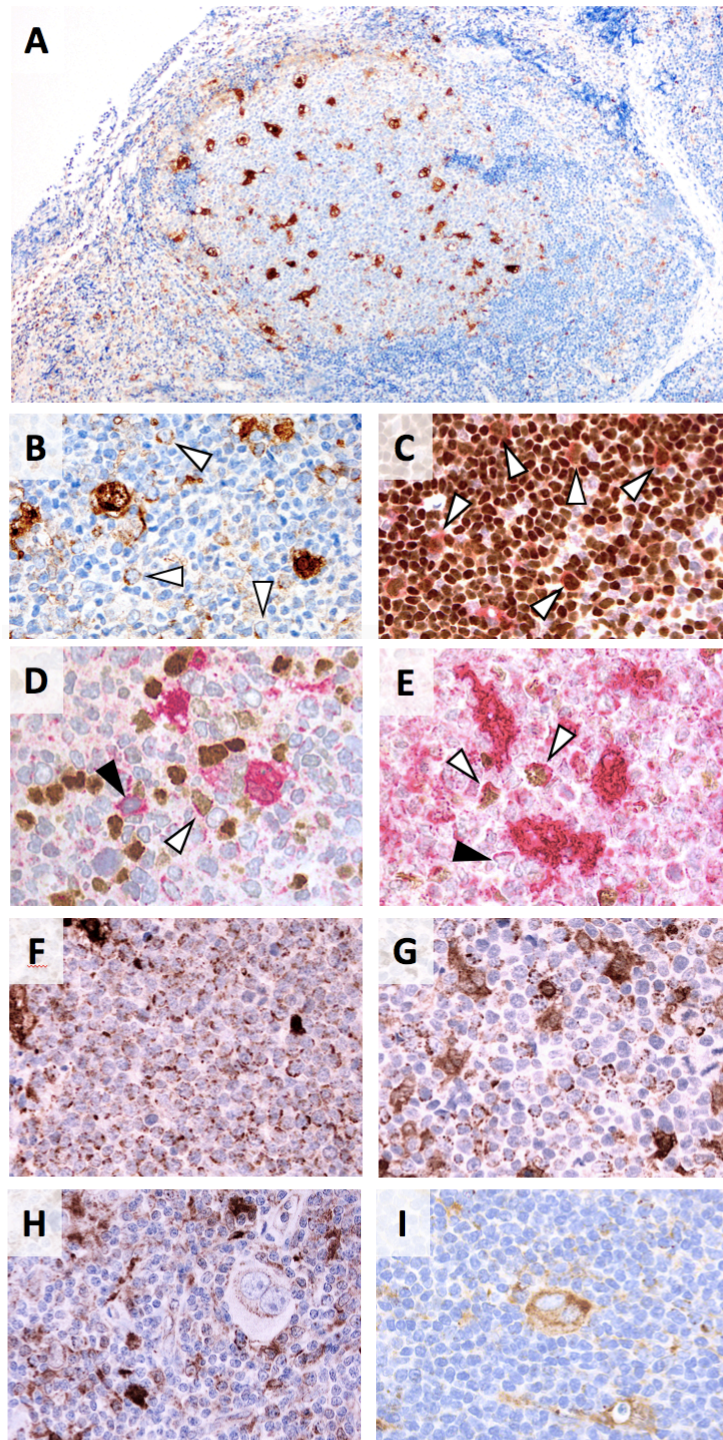
Figure 5. TRAP1 expression in non-neoplastic and neoplastic lymphoid cells.
A-E. In reactive lymphoid tissues, TRAP1 expression was observed in scattered GC blasts and in histiocytes; perifollicular lymphoid cells were TRAP1-negative (**A-B**). Double immunostaining for TRAP1 (*red*) and PAX5 (*brown*) (**C**) disclosed the B-cell nature of GC blasts. In particular, double immunostaining for TRAP1 (*red*) and IRF4 (*brown*) (**D**) and for TRAP1 (*red*) and c-Myc (*brown*) (**E**) highlighted TRAP1 expression in both re-cycling GC blasts (panel D, black arrowhead; panel E, white arrowheads) and plasma cell differentiating blasts (panel D, white arrowhead; panel E, black arrowhead). **G-I.** TRAP1 was diffusely expressed in the neoplastic cells of BL (**F**), DLBCL (**G**), cHL (bi-nucleated Reed-Sternberg and mononuclear Hodgkin cells) (**H**) and NLPHL (LP cells) (**I**). Non-

neoplastic by-stander cells disclosed variable degrees of TRAP1 positivity (Immunoperoxidase and phosphatase stains; original magnification, 5x, 20x and 40x).
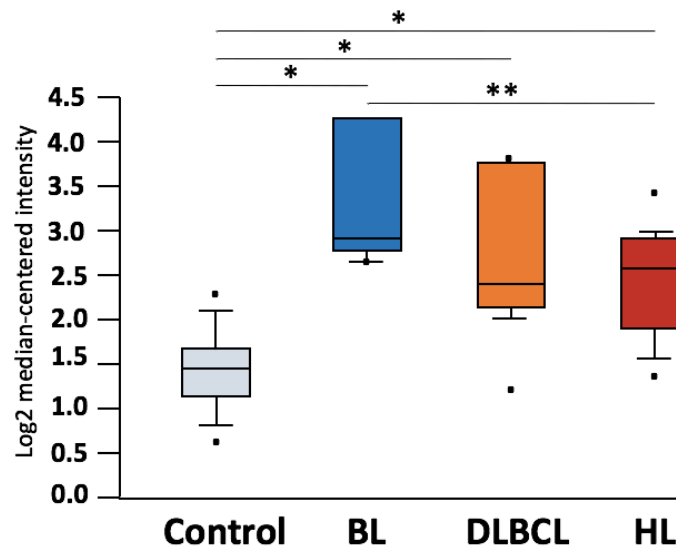

Figure 6. *In silico* gene expression profiles of TRAP1 mRNA in GC-derived B-cell lymphomas.
In silico gene expression profiles from the Oncomine database disclosed significantly higher TRAP1 mRNA expression levels in Burkitt lymphoma (BL), diffuse large B-cell lymphoma (DLBCL) and Hodgkin lymphomas (HL) compared to non-neoplastic control B-cells. The data shown in these figure refers to ref.102 (single asterisk, $p < 0.0001$; double asterisk, $p < 0.05$).

TRAP1 mRNA expression was assessed by *in silico* gene expression analysis, through the Oncomine database (106). These search highlighted *TRAP1* up-regulation in BL, DLBCL and HL compared to control (*i.e.* non-neoplastic) B-cells and other lymphoma entities ($p < 0.05$) (Figure 6). Of note, in all the available data sets, BL was associated with the highest *TRAP1* mRNA levels.

Moving from these *in silico* data, TRAP1 protein expression was investigated in representative primary samples of BL, DLBCL (both GCB and non-GCB type) and HL. In keeping with the gene expression analysis, TRAP1 was strongly and diffusely expressed in all BLs and in the vast majority of DLBCLs (32/33 cases [96.7%]), although with different intensity (from >80% to 40% of neoplastic cells) (Figure 5F-G). In DLBCL, the intensity and distribution of TRAP1 did not clearly correlate with a CGB or non-GCB phenotype. The protein was also strongly expressed in the neoplastic elements of both cHL (HRS cells) and NLPHL (LP cells) (Figure 5H-I).

5. DISCUSSION

The study of tumor cell biology largely relies on *in vivo* and *in vitro* models, recapitulating the basic molecular features of human neoplasms. This approach is instrumental to understand cancer biology, as it allows the characterization and genetic manipulation of homogeneous cell populations, while working in standardized experimental conditions. These advantages may nonetheless limit the clinical application of basic research studies, as human tumors are often much more complex than their *in vitro*/*in vivo* counterparts (109, 110).

Moving from these premises, the present project aimed to integrate the results of *in vitro* and *in vivo* studies on TRAP1-related oncogenesis (46, 64) with a thorough histological characterization of primary human samples. This led to compare the morphological and immunohistochemical features of primary human neoplasms and animal tumor models, also disclosing novel fields for the study of TRAP1-related oncogenic cascades.

The histological characterization of NF1-related peripheral nerve sheath tumors provided unprecedented information on the up-regulation of TRAP1 and its down-stream targets. In particular, it disclosed a progressive increase of TRAP1 expression from non-neoplastic tissues (*i.e.* peripheral nerve trunks) to PNs and MPNSTs. This finding is in line with what observed in other tumor models (*e.g.* TRAP1-related hepatocellular carcinogenesis) (61) and its consistency across animal species supports the oncogenic relevance of TRAP1-related metabolic reprogramming. In particular, immunohistochemical analysis confirmed the biological validity of prior *in vitro* oncogenic studies on *Nf1*-silenced stromal cells, which disclosed a pseudo-neoplastic phenotype as a consequence of MAPK pathway up-regulation, pERK1/2-mediated TRAP1 phosphorylation and HIF1α stabilization (46).

Quite notably, histological studies disclosed a diversified up-regulation of HIF1 target genes. Both human samples and animal tumor models indeed demonstrated a higher expression of PKM2 as compared to other proteins involved in glucose metabolism (*e.g.* GLUT1 and HK2) (Figure 3A). The reasons for such a difference are largely unknown, but the biochemical properties of PKM2 may provide a biological rationale for its more consistent up-regulation.

PKM2 is a tumor-specific variant of the last enzyme of the glycolytic pathway (pyruvate kinase [PK]). Compared to other PK variants, it has a reduced catalytic activity and is inhibited by growth factor-dependent signaling pathways (111, 112). As such, PKM2-expressing tumors are characterized by a reduced funneling of the glycolytic flow towards the TCA cycle and by the accumulation of metabolic intermediates that can be diverted into anabolic pathways (22). The unique features of PMK2 and the metabolic consequences of its over-expression are thus likely sufficient to provide tumor cells with an anabolic phenotype and may largely vicariate the limited up-regulation of glucose transporters (*e.g.* GLUT1) and/or other glycolytic enzymes (*e.g.* HK2). Furthermore, PKM2 contributes to the metabolic reprogramming of tumor cells by directly binding and co-activating HIF1 (113). All of these features possibly justify the prominent up-regulation of this enzyme, as compared with other glucose metabolism-related genes.

Morphometric and immunohistochemical studies on engineered mouse models also contributed to highlight the importance of TRAP1 in PN and MPNST oncogenesis. In particular, morphometric analyses disclosed a reduced size for shTRAP1 PNs compared to wild-type tumors (Figure 3B). This limited growing potential was not observed in shTRAP1 MPNSTs, suggesting the existence of TRAP1-independent oncogenic pathways that propel malignant tumor cell proliferation. Of note, TRAP1 silencing was associated with a reduced expression of HIF1α, its downstream targets (*e.g.* GLUT1, HK2 and PKM2) and GLUL. Taken together, these results may suggest a role for TRAP1 in glucose and glutamine metabolic reprogramming and in the acquisition of a fully neoplastic phenotype . Further *in vitro* and *in vivo* studies are need to confirm these histological data.

Immunohistochemical analysis was also applied to xenograft models of NF1-related MPNSTs (*i.e.* PDTXs and murine xenograft of the immortalized cysMPNST cell line). While the morphological and immunohistochemical features of PDTXs overlapped those of primary human samples and engineered mice, cisMPNST xenografts partially diverge from them. This inconsistency is likely related to the aberrant phenotypic and molecular features, which typically characterize immortalized cell lines as compared to their human counterpart (110). This drawback should limit the use of such model in future metabolic studies. Nonetheless, the subcutaneous injection of immortalized cisMPNST cells proved instrumental to assess the behavior and limited metastatic potential of heterotopic xenografts of NF1-related peripheral nerve sheath tumors.

With respect to the hematological branch of this study, histological analysis contributed to expand the spectrum of TRAP1-expressing human neoplasms. Prior studies on TRAP1-related oncogenic cascades indeed focused on solid tumor models (46, 61, 114-117), while little (if any) information was available on TRAP1 expression in lymphoproliferative disorders. Moving from a thorough phenotypic characterization of reactive lymphoid tissues, this study highlighted TRAP1 expression in non-neoplastic re-cycling and differentiating GC blasts, in GC-derived high-grade B-cell lymphomas (*i.e.* BL and DLBCL) and in the neoplastic blasts (*i.e.* HRS and LP cells) of HL.

From a pathogenic viewpoint, TRAP1 expression in such lymphomas may stem: (i) from the protein constitutive positivity in their non-neoplastic counterparts; and/or (ii) from disease-specific molecular derangements. In fact, some evidence suggests that c-Myc directly binds *TRAP1* promoter and induces its over-expression (118). Of note, virtually all BLs and HLs and a consistent subset of DLBCLs are characterized by moderate to high c-Myc expression levels, as a result of recurrent chromosomal translocations (BL and some DLBCLs) or disease-specific gene expression profiles (HL and subsets of DLBCL) (81, 119). In such tumors, it is thus possible that TRAP1 positivity directly stems from the constitutive expression of c-Myc. Taken together, these data suggest a complex molecular scenario, whereby TRAP1 over-expression in GC-derived B-cell lymphomas may

depend on the tumor origin (*i.e.* TRAP1-expressing GC blasts) as well as on disease-specific genetic derangements. This is further sustained by the variability of TRAP1-positive cells among DLBCLs.

DLBCLs are very heterogeneous neoplasms, characterized by distinct molecular and metabolic features. Gene expression studies have indeed highlighted the existence of metabolically diverse sub-groups, relying on either oxidative phosphorylation (*i.e* OxPhos signature) or aerobic glycolysis (*i.e.* BCR signature) for their energetic needs (91). The OxPhos signature is characterized by the hyper-expression of respiratory chain components (*e.g.* complex I and complex II), ATP synthase and pyruvate dehydrogenase subunits and several TCA cycle enzymes. By contrast, the BCR signature is associated with reduced mitochondrial respiration and fatty acid oxidation and with increased glycolytic flux (120). These data may explain the variability of TRAP1 expression among DLBCLs. In fact, those cases with enhanced glycolytic features (*i.e.* BCR signature) may be associated with TRAP1 over-expression. By contrast, the OxPhos signature putatively relies on TRAP1-unrelated metabolic programs and may include cases with reduced TRAP1 expression. Further genetic and molecular studies are needed to test this hypothesis and to investigate any possible correlation between TRAP1 expression and the metabolic features of DLBCL.

6. CONCLUSIONS

This study highlights the contribution of histology to the understanding of tumor metabolism. Morphological and immunohistochemical analyses integrate the results of *in vitro* and *in vivo* studies and identify novel fields for tumor metabolic investigations.

In particular, histology confirms the relevance of TRAP1 activation in NF1-related peripheral nerve sheath tumors and discloses a tight correspondence between the pathological (*i.e.* morphological) features of primary human samples and animal tumor models. Immunohistochemical characterization of reactive lymphoid tissues and primary lymphoma samples also identifies recurrent TRAP1 expression profiles, possibly subtending tumor-related metabolic networks.

7. REFERENCES

1.   Hanahan D, Weinberg RA. Hallmarks of cancer: the next generation. Cell 2011; 144, 646-674.

2.   Berdasco M, Esteller M. Aberrant epigenetic landscape in cancer: how cellular identity goes awry. Dev Cell 2010; 19, 698-711.

3.   Ciccia A, Elledge SJ. The DNA damage response: making it safe to play with knives. Mol Cell 2010; 40, 179-204.

4.   Lin KW, Yan J. The telomere length dynamic and methods of its assessment. J Cell Mol Med 2005; 9, 977-989.

5.   Quail DF, Joyce JA. Microenvironmental regulation of tumor progression and metastasis. Nat Med 2013; 19, 1423-1437.

6.   Pizzi M, Boi M, Bertoni F, Inghirami G. Emerging therapies provide new opportunities to reshape the multifaceted interactions between the immune system and lymphoma cells. Leukemia 2016; 30, 1805-1815.

7.   Candido J, Hagemann T. Cancer-related inflammation. J Clin Immunol 2013; 33 Suppl 1, S79-84.

8.   Landskron G, De la Fuente M, Thuwajit P, Thuwajit C, Hermoso MA. Chronic inflammation and cytokines in the tumor microenvironment. J Immunol Res 2014; 2014, 149185.

9.   Pizzi M, Margolskee E, Inghirami G. Pathogenesis of Peripheral T Cell Lymphoma. Annu Rev Pathol 2018; 13, 293-320.

10.   Martin GS. Cell signaling and cancer. Cancer Cell 2003; 4, 167-174.

11.   Sherr CJ, McCormick F. The RB and p53 pathways in cancer. Cancer Cell 2002; 2, 103-112.

12.   Petrilli AM, Fernandez-Valle C. Role of Merlin/NF2 inactivation in tumor biology. Oncogene 2016; 35, 537-548.

13.   Wong RS. Apoptosis in cancer: from pathogenesis to treatment. J Exp Clin Cancer Res 2011; 30, 87.

14.   Wang Y, Xie J, Wang H, Huang H, Xie P. Beclin-1 suppresses gastric cancer progression by promoting apoptosis and reducing cell migration. Oncol Lett 2017; 14, 6857-6862.

15.   Rohatgi RA, Shaw LM. An autophagy-independent function for Beclin 1 in cancer. Mol Cell Oncol 2016; 3.

16.   Jafri MA, Ansari SA, Alqahtani MH, Shay JW. Roles of telomeres and telomerase in cancer, and advances in telomerase-targeted therapies. Genome Med 2016; 8, 69.

17.   Park JI, Venteicher AS, Hong JY, Choi J, Jun S, Shkreli M, Chang W, Meng Z, Cheung P, Ji H, McLaughlin M, Veenstra TD, Nusse R, McCrea PD, Artandi SE. Telomerase modulates Wnt signalling by association with target gene chromatin. Nature 2009; 460, 66-72.

18.   Masutomi K, Possemato R, Wong JM, Currier JL, Tothova Z, Manola JB, Ganesan S, Lansdorp PM, Collins K, Hahn WC. The telomerase reverse transcriptase regulates chromatin state and DNA damage responses. Proc Natl Acad Sci U S A 2005; 102, 8222-8227.

19.   Heaphy CM, de Wilde RF, Jiao Y, Klein AP, Edil BH, Shi C, Bettegowda C, Rodriguez FJ, Eberhart CG, Hebbar S, Offerhaus GJ, McLendon R, Rasheed BA, He Y, Yan H, Bigner DD, Oba-Shinjo SM, Marie SK, Riggins GJ, Kinzler KW, Vogelstein B, Hruban RH, Maitra A, Papadopoulos N, Meeker AK. Altered telomeres in tumors with ATRX and DAXX mutations. Science 2011; 333, 425.

20.   Chen HF, Wu KJ. Endothelial Transdifferentiation of Tumor Cells Triggered by the Twist1-Jagged1-KLF4 Axis: Relationship between Cancer Stemness and Angiogenesis. Stem Cells Int 2016; 2016, 6439864.

21.   Patenaude A, Parker J, Karsan A. Involvement of endothelial progenitor cells in tumor vascularization. Microvasc Res 2010; 79, 217-223.

22.   Pavlova NN, Thompson CB. The Emerging Hallmarks of Cancer Metabolism. Cell Metab 2016; 23, 27-47.

23.   Yanagida O, Kanai Y, Chairoungdua A, Kim DK, Segawa H, Nii T, Cha SH, Matsuo H, Fukushima J, Fukasawa Y, Tani Y, Taketani Y, Uchino H, Kim JY, Inatomi J, Okayasu I, Miyamoto K, Takeda E, Goya T, Endou H. Human L-type amino acid transporter 1 (LAT1): characterization of function and expression in tumor cell lines. Biochim Biophys Acta 2001; 1514, 291-302.

24.   Wieman HL, Wofford JA, Rathmell JC. Cytokine stimulation promotes glucose uptake via phosphatidylinositol-3 kinase/Akt regulation of Glut1 activity and trafficking. Mol Biol Cell 2007; 18, 1437-1446.

25.   Gao P, Tchernyshyov I, Chang TC, Lee YS, Kita K, Ochi T, Zeller KI, De Marzo AM, Van Eyk JE, Mendell JT, Dang CV. c-Myc suppression of miR-23a/b enhances mitochondrial glutaminase expression and glutamine metabolism. Nature 2009; 458, 762-765.

26.   Gottlob K, Majewski N, Kennedy S, Kandel E, Robey RB, Hay N. Inhibition of early apoptotic events by Akt/PKB is dependent on the first committed step of glycolysis and mitochondrial hexokinase. Genes Dev 2001; 15, 1406-1418.

27.   Gao JY, Song BR, Peng JJ, Lu YM. Correlation between mitochondrial TRAP-1 expression and lymph node metastasis in colorectal cancer. World J Gastroenterol 2012; 18, 5965-5971.

28.   Kerr MC, Teasdale RD. Defining macropinocytosis. Traffic 2009; 10, 364-371.

29.   Krajcovic M, Krishna S, Akkari L, Joyce JA, Overholtzer M. mTOR regulates phagosome and entotic vacuole fission. Mol Biol Cell 2013; 24, 3736-3745.

30.   Boya P, Reggiori F, Codogno P. Emerging regulation and functions of autophagy. Nat Cell Biol 2013; 15, 713-720.

31.   Liberti MV, Locasale JW. The Warburg Effect: How Does it Benefit Cancer Cells? Trends Biochem Sci 2016; 41, 211-218.

32.   Wellen KE, Lu C, Mancuso A, Lemons JM, Ryczko M, Dennis JW, Rabinowitz JD, Coller HA, Thompson CB. The hexosamine biosynthetic pathway couples growth factor-induced glutamine uptake to glucose metabolism. Genes Dev 2010; 24, 2784-2799.

33.   Locasale JW, Grassian AR, Melman T, Lyssiotis CA, Mattaini KR, Bass AJ, Heffron G, Metallo CM, Muranen T, Sharfi H, Sasaki AT, Anastasiou D, Mullarky E, Vokes NI, Sasaki M, Beroukhim R, Stephanopoulos G, Ligon AH, Meyerson M, Richardson AL, Chin L, Wagner G, Asara JM, Brugge JS, Cantley LC, Vander Heiden MG. Phosphoglycerate dehydrogenase diverts glycolytic flux and contributes to oncogenesis. Nat Genet 2011; 43, 869-874.

34.   Bauer DE, Hatzivassiliou G, Zhao F, Andreadis C, Thompson CB. ATP citrate lyase is an important component of cell growth and transformation. Oncogene 2005; 24, 6314-6322.

35.   Sullivan LB, Gui DY, Hosios AM, Bush LN, Freinkman E, Vander Heiden MG. Supporting Aspartate Biosynthesis Is an Essential Function of Respiration in Proliferating Cells. Cell 2015; 162, 552-563.

36.   Zhang J, Pavlova NN, Thompson CB. Cancer cell metabolism: the essential role of the nonessential amino acid, glutamine. EMBO J 2017; 36, 1302-1315.

37.   Kim JW, Tchernyshyov I, Semenza GL, Dang CV. HIF-1-mediated expression of pyruvate dehydrogenase kinase: a metabolic switch required for cellular adaptation to hypoxia. Cell Metab 2006; 3, 177-185.

38.   Wahlstrom T, Henriksson MA. Impact of MYC in regulation of tumor cell metabolism. Biochim Biophys Acta 2015; 1849, 563-569.

39.   Cai L, Sutter BM, Li B, Tu BP. Acetyl-CoA induces cell growth and proliferation by promoting the acetylation of histones at growth genes. Mol Cell 2011; 42, 426-437.

40.   Sabari BR, Tang Z, Huang H, Yong-Gonzalez V, Molina H, Kong HE, Dai L, Shimada M, Cross JR, Zhao Y, Roeder RG, Allis CD. Intracellular crotonyl-CoA stimulates transcription through p300-catalyzed histone crotonylation. Mol Cell 2015; 58, 203-215.

41.   Towbin BD, Gonzalez-Aguilera C, Sack R, Gaidatzis D, Kalck V, Meister P, Askjaer P, Gasser SM. Step-wise methylation of histone H3K9 positions heterochromatin at the nuclear periphery. Cell 2012; 150, 934-947.

42.   Fischer K, Hoffmann P, Voelkl S, Meidenbauer N, Ammer J, Edinger M, Gottfried E, Schwarz S, Rothe G, Hoves S, Renner K, Timischl B, Mackensen A, Kunz-Schughart L, Andreesen R, Krause SW, Kreutz M. Inhibitory effect of tumor cell-derived lactic acid on human T cells. Blood 2007; 109, 3812-3819.

43.   Carmona-Fontaine C, Bucci V, Akkari L, Deforet M, Joyce JA, Xavier JB. Emergence of spatial structure in the tumor microenvironment due to the Warburg effect. Proc Natl Acad Sci U S A 2013; 110, 19402-19407.

44.   Rothberg JM, Bailey KM, Wojtkowiak JW, Ben-Nun Y, Bogyo M, Weber E, Moin K, Blum G, Mattingly RR, Gillies RJ, Sloane BF. Acid-mediated tumor proteolysis: contribution of cysteine cathepsins. Neoplasia 2013; 15, 1125-1137.

45.   Fallarino F, Grohmann U, You S, McGrath BC, Cavener DR, Vacca C, Orabona C, Bianchi R, Belladonna ML, Volpi C, Santamaria P, Fioretti MC, Puccetti P. The combined effects of tryptophan starvation and tryptophan catabolites down-regulate T cell receptor zeta-chain and induce a regulatory phenotype in naive T cells. J Immunol 2006; 176, 6752-6761.

46.   Masgras I, Ciscato F, Brunati AM, Tibaldi E, Indraccolo S, Curtarello M, Chiara F, Cannino G, Papaleo E, Lambrughi M, Guzzo G, Gambalunga A, Pizzi M, Guzzardo V, Rugge M, Vuljan SE, Calabrese F, Bernardi P, Rasola A. Absence of Neurofibromin Induces an Oncogenic Metabolic

Switch via Mitochondrial ERK-Mediated Phosphorylation of the Chaperone TRAP1. Cell Rep 2017; 18, 659-672.

47.   Kang BH. TRAP1 regulation of mitochondrial life or death decision in cancer cells and mitochondria-targeted TRAP1 inhibitors. BMB Rep 2012; 45, 1-6.

48.   Partridge JR, Lavery LA, Elnatan D, Naber N, Cooke R, Agard DA. A novel N-terminal extension in mitochondrial TRAP1 serves as a thermal regulator of chaperone activity. Elife 2014; 3.

49.   Lavery LA, Partridge JR, Ramelot TA, Elnatan D, Kennedy MA, Agard DA. Structural asymmetry in the closed state of mitochondrial Hsp90 (TRAP1) supports a two-step ATP hydrolysis mechanism. Mol Cell 2014; 53, 330-343.

50.   Leskovar A, Wegele H, Werbeck ND, Buchner J, Reinstein J. The ATPase cycle of the mitochondrial Hsp90 analog Trap1. J Biol Chem 2008; 283, 11677-11688.

51.   Sung N, Lee J, Kim JH, Chang C, Joachimiak A, Lee S, Tsai FT. Mitochondrial Hsp90 is a ligand-activated molecular chaperone coupling ATP binding to dimer closure through a coiled-coil intermediate. Proc Natl Acad Sci U S A 2016; 113, 2952-2957.

52.   Hassan MA, Tolba OA. Iron chelation monotherapy in transfusion-dependent beta-thalassemia major patients: a comparative study of deferasirox and deferoxamine. Electron Physician 2016; 8, 2425-2431.

53.   Montesano Gesualdi N, Chirico G, Pirozzi G, Costantino E, Landriscina M, Esposito F. Tumor necrosis factor-associated protein 1 (TRAP-1) protects cells from oxidative stress and apoptosis. Stress 2007; 10, 342-350.

54.   Bernardi P, Rasola A, Forte M, Lippe G. The Mitochondrial Permeability Transition Pore: Channel Formation by F-ATP Synthase, Integration in Signal Transduction, and Role in Pathophysiology. Physiol Rev 2015; 95, 1111-1155.

55.   Ghosh JC, Siegelin MD, Dohi T, Altieri DC. Heat shock protein 60 regulation of the mitochondrial permeability transition pore in tumor cells. Cancer Res 2010; 70, 8988-8993.

56.   Guzzo G, Sciacovelli M, Bernardi P, Rasola A. Inhibition of succinate dehydrogenase by the mitochondrial chaperone TRAP1 has anti-oxidant and anti-apoptotic effects on tumor cells. Oncotarget 2014; 5, 11897-11908.

57.   Masgras I, Sanchez-Martin C, Colombo G, Rasola A. The Chaperone TRAP1 As a Modulator of the Mitochondrial Adaptations in Cancer Cells. Front Oncol 2017; 7, 58.

58.   Pridgeon JW, Olzmann JA, Chin LS, Li L. PINK1 protects against oxidative stress by phosphorylating mitochondrial chaperone TRAP1. PLoS Biol 2007; 5, e172.

59.   Yoshida S, Tsutsumi S, Muhlebach G, Sourbier C, Lee MJ, Lee S, Vartholomaiou E, Tatokoro M, Beebe K, Miyajima N, Mohney RP, Chen Y, Hasumi H, Xu W, Fukushima H, Nakamura K, Koga F, Kihara K, Trepel J, Picard D, Neckers L. Molecular chaperone TRAP1 regulates a metabolic switch between mitochondrial respiration and aerobic glycolysis. Proc Natl Acad Sci U S A 2013; 110, E1604-1612.

60.   Vyas S, Zaganjor E, Haigis MC. Mitochondria and Cancer. Cell 2016; 166, 555-566.

61.   Kowalik MA, Guzzo G, Morandi A, Perra A, Menegon S, Masgras I, Trevisan E, Angioni MM, Fornari F, Quagliata L, Ledda-Columbano GM, Gramantieri L, Terracciano L, Giordano S, Chiarugi P, Rasola A, Columbano A. Metabolic reprogramming identifies the most aggressive lesions at early phases of hepatic carcinogenesis. Oncotarget 2016; 7, 32375-32393.

62.   Zhang B, Wang J, Huang Z, Wei P, Liu Y, Hao J, Zhao L, Zhang F, Tu Y, Wei T. Aberrantly upregulated TRAP1 is required for tumorigenesis of breast cancer. Oncotarget 2015; 6, 44495-44508.

63.   Agorreta J, Hu J, Liu D, Delia D, Turley H, Ferguson DJ, Iborra F, Pajares MJ, Larrayoz M, Zudaire I, Pio R, Montuenga LM, Harris AL, Gatter K, Pezzella F. TRAP1 regulates proliferation, mitochondrial function, and has prognostic significance in NSCLC. Mol Cancer Res 2014; 12, 660-669.

64.   Sciacovelli M, Guzzo G, Morello V, Frezza C, Zheng L, Nannini N, Calabrese F, Laudiero G, Esposito F, Landriscina M, Defilippi P, Bernardi P, Rasola A. The mitochondrial chaperone TRAP1 promotes neoplastic growth by inhibiting succinate dehydrogenase. Cell Metab 2013; 17, 988-999.

65.   Lisanti S, Tavecchio M, Chae YC, Liu Q, Brice AK, Thakur ML, Languino LR, Altieri DC. Deletion of the mitochondrial chaperone TRAP-1 uncovers global reprogramming of metabolic networks. Cell Rep 2014; 8, 671-677.

66.   Masoud GN, Li W. HIF-1alpha pathway: role, regulation and intervention for cancer therapy. Acta Pharm Sin B 2015; 5, 378-389.

67.   Chae YC, Caino MC, Lisanti S, Ghosh JC, Dohi T, Danial NN, Villanueva J, Ferrero S, Vaira V, Santambrogio L, Bosari S, Languino LR, Herlyn M, Altieri DC. Control of tumor bioenergetics and survival stress signaling by mitochondrial HSP90s. Cancer Cell 2012; 22, 331-344.

68.   Fouad YA, Aanei C. Revisiting the hallmarks of cancer. Am J Cancer Res 2017; 7, 1016-1036.

69.   Rodriguez FJ, Stratakis CA, Evans DG. Genetic predisposition to peripheral nerve neoplasia: diagnostic criteria and pathogenesis of neurofibromatoses, Carney complex, and related syndromes. Acta Neuropathol 2012; 123, 349-367.

70.   Gutmann DH, Aylsworth A, Carey JC, Korf B, Marks J, Pyeritz RE, Rubenstein A, Viskochil D. The diagnostic evaluation and multidisciplinary management of neurofibromatosis 1 and neurofibromatosis 2. JAMA 1997; 278, 51-57.

71.   Louis DN, Ohgaki H, Wiestler OD, Cavenee WK, World Health Organization, International Agency for Research on Cancer. WHO classification of tumours of the central nervous system. Lyon: International Agency For Research On Cancer, 2016.

72.   De Raedt T, Brems H, Wolkenstein P, Vidaud D, Pilotti S, Perrone F, Mautner V, Frahm S, Sciot R, Legius E. Elevated risk for MPNST in NF1 microdeletion patients. Am J Hum Genet 2003; 72, 1288-1292.

73.   Pasmant E, Sabbagh A, Spurlock G, Laurendeau I, Grillo E, Hamel MJ, Martin L, Barbarot S, Leheup B, Rodriguez D, Lacombe D, Dollfus H, Pasquier L, Isidor B, Ferkal S, Soulier J, Sanson M, Dieux-Coeslier A, Bieche I, Parfait B, Vidaud M, Wolkenstein P, Upadhyaya M, Vidaud D, members of the NFFN. NF1 microdeletions in neurofibromatosis type 1: from genotype to phenotype. Hum Mutat 2010; 31, E1506-1518.

74.   Fletcher CDM, World Health Organization., International Agency for Research on Cancer. WHO classification of tumours of soft tissue and bone. Lyon: IARC Press, 2013.

75.   Schaefer IM, Fletcher CD. Malignant peripheral nerve sheath tumor (MPNST) arising in diffuse-type neurofibroma: clinicopathologic characterization in a series of 9 cases. Am J Surg Pathol 2015; 39, 1234-1241.

76.   Kluwe L, Friedrich RE, Mautner VF. Allelic loss of the NF1 gene in NF1-associated plexiform neurofibromas. Cancer Genet Cytogenet 1999; 113, 65-69.

77.   Storlazzi CT, Von Steyern FV, Domanski HA, Mandahl N, Mertens F. Biallelic somatic inactivation of the NF1 gene through chromosomal translocations in a sporadic neurofibroma. Int J Cancer 2005; 117, 1055-1057.

78.   McCaughan JA, Holloway SM, Davidson R, Lam WW. Further evidence of the increased risk for malignant peripheral nerve sheath tumour from a Scottish cohort of patients with neurofibromatosis type 1. J Med Genet 2007; 44, 463-466.

79.   Margueron R, Reinberg D. The Polycomb complex PRC2 and its mark in life. Nature 2011; 469, 343-349.

80.   Lee W, Teckie S, Wiesner T, Ran L, Prieto Granada CN, Lin M, Zhu S, Cao Z, Liang Y, Sboner A, Tap WD, Fletcher JA, Huberman KH, Qin LX, Viale A, Singer S, Zheng D, Berger MF, Chen Y, Antonescu CR, Chi P. PRC2 is recurrently inactivated through EED or SUZ12 loss in malignant peripheral nerve sheath tumors. Nat Genet 2014; 46, 1227-1232.

81.   Swerdlow SH, World Health Organization, International Agency for Research on Cancer. WHO classification of tumours of haematopoietic and lymphoid tissues. Lyon: International Agency for Research on Cancer, 2017.

82.   Basso K, Dalla-Favera R. Germinal centres and B cell lymphomagenesis. Nat Rev Immunol 2015; 15, 172-184.

83.   De Silva NS, Klein U. Dynamics of B cells in germinal centres. Nat Rev Immunol 2015; 15, 137-148.

84.   Dominguez-Sola D, Victora GD, Ying CY, Phan RT, Saito M, Nussenzweig MC, Dalla-Favera R. The proto-oncogene MYC is required for selection in the germinal center and cyclic reentry. Nat Immunol 2012; 13, 1083-1091.

85.   Nutt SL, Hodgkin PD, Tarlinton DM, Corcoran LM. The generation of antibody-secreting plasma cells. Nat Rev Immunol 2015; 15, 160-171.

86.   Freedman A. Follicular lymphoma: 2018 update on diagnosis and management. Am J Hematol 2018; 93, 296-305.

87.   Link BK, Maurer MJ, Nowakowski GS, Ansell SM, Macon WR, Syrbu SI, Slager SL, Thompson CA, Inwards DJ, Johnston PB, Colgan JP, Witzig TE, Habermann TM, Cerhan JR. Rates and outcomes of follicular lymphoma transformation in the immunochemotherapy era: a report from the University of Iowa/MayoClinic Specialized Program of Research Excellence Molecular Epidemiology Resource. J Clin Oncol 2013; 31, 3272-3278.

88.   Victora GD, Dominguez-Sola D, Holmes AB, Deroubaix S, Dalla-Favera R, Nussenzweig MC. Identification of human germinal center light and dark zone cells and their relationship to human B-cell lymphomas. Blood 2012; 120, 2240-2248.

89.   Alizadeh AA, Eisen MB, Davis RE, Ma C, Lossos IS, Rosenwald A, Boldrick JC, Sabet H, Tran T, Yu X, Powell JI, Yang L, Marti GE, Moore T, Hudson J, Jr., Lu L, Lewis DB, Tibshirani R, Sherlock G, Chan WC, Greiner TC, Weisenburger DD, Armitage JO, Warnke R, Levy R, Wilson W, Grever MR, Byrd JC, Botstein D, Brown PO, Staudt LM. Distinct types of diffuse large B-cell lymphoma identified by gene expression profiling. Nature 2000; 403, 503-511.

90.   Hans CP, Weisenburger DD, Greiner TC, Gascoyne RD, Delabie J, Ott G, Muller-Hermelink HK, Campo E, Braziel RM, Jaffe ES, Pan Z, Farinha P, Smith LM, Falini B, Banham AH, Rosenwald

A, Staudt LM, Connors JM, Armitage JO, Chan WC. Confirmation of the molecular classification of diffuse large B-cell lymphoma by immunohistochemistry using a tissue microarray. Blood 2004; 103, 275-282.

91.   Monti S, Savage KJ, Kutok JL, Feuerhake F, Kurtin P, Mihm M, Wu B, Pasqualucci L, Neuberg D, Aguiar RC, Dal Cin P, Ladd C, Pinkus GS, Salles G, Harris NL, Dalla-Favera R, Habermann TM, Aster JC, Golub TR, Shipp MA. Molecular profiling of diffuse large B-cell lymphoma identifies robust subtypes including one characterized by host inflammatory response. Blood 2005; 105, 1851-1861.

92.   Reddy A, Zhang J, Davis NS, Moffitt AB, Love CL, Waldrop A, Leppa S, Pasanen A, Meriranta L, Karjalainen-Lindsberg ML, Norgaard P, Pedersen M, Gang AO, Hogdall E, Heavican TB, Lone W, Iqbal J, Qin Q, Li G, Kim SY, Healy J, Richards KL, Fedoriw Y, Bernal-Mizrachi L, Koff JL, Staton AD, Flowers CR, Paltiel O, Goldschmidt N, Calaminici M, Clear A, Gribben J, Nguyen E, Czader MB, Ondrejka SL, Collie A, Hsi ED, Tse E, Au-Yeung RKH, Kwong YL, Srivastava G, Choi WWL, Evens AM, Pilichowska M, Sengar M, Reddy N, Li S, Chadburn A, Gordon LI, Jaffe ES, Levy S, Rempel R, Tzeng T, Happ LE, Dave T, Rajagopalan D, Datta J, Dunson DB, Dave SS. Genetic and Functional Drivers of Diffuse Large B Cell Lymphoma. Cell 2017; 171, 481-494 e415.

93.   Chapuy B, Stewart C, Dunford AJ, Kim J, Kamburov A, Redd RA, Lawrence MS, Roemer MGM, Li AJ, Ziepert M, Staiger AM, Wala JA, Ducar MD, Leshchiner I, Rheinbay E, Taylor-Weiner A, Coughlin CA, Hess JM, Pedamallu CS, Livitz D, Rosebrock D, Rosenberg M, Tracy AA, Horn H, van Hummelen P, Feldman AL, Link BK, Novak AJ, Cerhan JR, Habermann TM, Siebert R, Rosenwald A, Thorner AR, Meyerson ML, Golub TR, Beroukhim R, Wulf GG, Ott G, Rodig SJ, Monti S, Neuberg DS, Loeffler M, Pfreundschuh M, Trumper L, Getz G, Shipp MA. Molecular subtypes of diffuse large B cell lymphoma are associated with distinct pathogenic mechanisms and outcomes. Nat Med 2018; 24, 679-690.

94.   Schmitz R, Wright GW, Huang DW, Johnson CA, Phelan JD, Wang JQ, Roulland S, Kasbekar M, Young RM, Shaffer AL, Hodson DJ, Xiao W, Yu X, Yang Y, Zhao H, Xu W, Liu X, Zhou B, Du W, Chan WC, Jaffe ES, Gascoyne RD, Connors JM, Campo E, Lopez-Guillermo A, Rosenwald A, Ott G, Delabie J, Rimsza LM, Tay Kuang Wei K, Zelenetz AD, Leonard JP, Bartlett NL, Tran B, Shetty J, Zhao Y, Soppet DR, Pittaluga S, Wilson WH, Staudt LM. Genetics and Pathogenesis of Diffuse Large B-Cell Lymphoma. N Engl J Med 2018; 378, 1396-1407.

95.   Dalla-Favera R, Bregni M, Erikson J, Patterson D, Gallo RC, Croce CM. Human c-myc onc gene is located on the region of chromosome 8 that is translocated in Burkitt lymphoma cells. Proc Natl Acad Sci U S A 1982; 79, 7824-7827.

96.   Brady G, MacArthur GJ, Farrell PJ. Epstein-Barr virus and Burkitt lymphoma. J Clin Pathol 2007; 60, 1397-1402.

97.   Piccaluga PP, Agostinelli C, Gazzola A, Tripodo C, Bacci F, Sabattini E, Sista MT, Mannu C, Sapienza MR, Rossi M, Laginestra MA, Sagramoso-Sacchetti CA, Righi S, Pileri SA. Pathobiology of hodgkin lymphoma. Adv Hematol 2011; 2011, 920898.

98.   Smith LB. Nodular lymphocyte predominant Hodgkin lymphoma: diagnostic pearls and pitfalls. Arch Pathol Lab Med 2010; 134, 1434-1439.

99.   Fan Z, Natkunam Y, Bair E, Tibshirani R, Warnke RA. Characterization of variant patterns of nodular lymphocyte predominant hodgkin lymphoma with immunohistologic and clinical correlation. Am J Surg Pathol 2003; 27, 1346-1356.

100.   Brune V, Tiacci E, Pfeil I, Doring C, Eckerle S, van Noesel CJ, Klapper W, Falini B, von Heydebreck A, Metzler D, Brauninger A, Hansmann ML, Kuppers R. Origin and pathogenesis of nodular lymphocyte-predominant Hodgkin lymphoma as revealed by global gene expression analysis. J Exp Med 2008; 205, 2251-2268.

101.   Buettner M, Greiner A, Avramidou A, Jack HM, Niedobitek G. Evidence of abortive plasma cell differentiation in Hodgkin and Reed-Sternberg cells of classical Hodgkin lymphoma. Hematol Oncol 2005; 23, 127-132.

102.   Tiacci E, Doring C, Brune V, van Noesel CJ, Klapper W, Mechtersheimer G, Falini B, Kuppers R, Hansmann ML. Analyzing primary Hodgkin and Reed-Sternberg cells to capture the molecular and cellular pathogenesis of classical Hodgkin lymphoma. Blood 2012; 120, 4609-4620.

103.   Castellsague J, Gel B, Fernandez-Rodriguez J, Llatjos R, Blanco I, Benavente Y, Perez-Sidelnikova D, Garcia-Del Muro J, Vinals JM, Vidal A, Valdes-Mas R, Terribas E, Lopez-Doriga A, Pujana MA, Capella G, Puente XS, Serra E, Villanueva A, Lazaro C. Comprehensive establishment and characterization of orthoxenograft mouse models of malignant peripheral nerve sheath tumors for personalized medicine. EMBO Mol Med 2015; 7, 608-627.

104.   Chen Z, Liu C, Patel AJ, Liao CP, Wang Y, Le LQ. Cells of origin in the embryonic nerve roots for NF1-associated plexiform neurofibroma. Cancer Cell 2014; 26, 695-706.

105.   Pizzi M, Agostinelli C, Righi S, Gazzola A, Mannu C, Galuppini F, Fassan M, Visentin A, Piazza F, Semenzato GC, Rugge M, Sabattini E. Aberrant expression of CD10 and BCL6 in mantle cell lymphoma. Histopathology 2017; 71, 769-777.

106.   Rhodes DR, Yu J, Shanker K, Deshpande N, Varambally R, Ghosh D, Barrette T, Pandey A, Chinnaiyan AM. ONCOMINE: a cancer microarray database and integrated data-mining platform. Neoplasia 2004; 6, 1-6.

107.   Basso K, Margolin AA, Stolovitzky G, Klein U, Dalla-Favera R, Califano A. Reverse engineering of regulatory networks in human B cells. Nat Genet 2005; 37, 382-390.

108.   Compagno M, Lim WK, Grunn A, Nandula SV, Brahmachary M, Shen Q, Bertoni F, Ponzoni M, Scandurra M, Califano A, Bhagat G, Chadburn A, Dalla-Favera R, Pasqualucci L. Mutations of multiple genes cause deregulation of NF-kappaB in diffuse large B-cell lymphoma. Nature 2009; 459, 717-721.

109.   Katt ME, Placone AL, Wong AD, Xu ZS, Searson PC. In Vitro Tumor Models: Advantages, Disadvantages, Variables, and Selecting the Right Platform. Front Bioeng Biotechnol 2016; 4, 12.

110.   Pizzi M, Inghirami G. Patient-derived tumor xenografts of lymphoproliferative disorders: are they surrogates for the human disease? Curr Opin Hematol 2017; 24, 384-392.

111.   Christofk HR, Vander Heiden MG, Harris MH, Ramanathan A, Gerszten RE, Wei R, Fleming MD, Schreiber SL, Cantley LC. The M2 splice isoform of pyruvate kinase is important for cancer metabolism and tumour growth. Nature 2008; 452, 230-233.

112.   Christofk HR, Vander Heiden MG, Wu N, Asara JM, Cantley LC. Pyruvate kinase M2 is a phosphotyrosine-binding protein. Nature 2008; 452, 181-186.

113.   Luo W, Hu H, Chang R, Zhong J, Knabel M, O'Meally R, Cole RN, Pandey A, Semenza GL. Pyruvate kinase M2 is a PHD3-stimulated coactivator for hypoxia-inducible factor 1. Cell 2011; 145, 732-744.

114.   Barbosa IA, Vega-Naredo I, Loureiro R, Branco AF, Garcia R, Scott PM, Oliveira PJ. TRAP1 regulates autophagy in lung cancer cells. Eur J Clin Invest 2018; 48.

115.   Amoroso MR, Matassa DS, Agliarulo I, Avolio R, Maddalena F, Condelli V, Landriscina M, Esposito F. Stress-Adaptive Response in Ovarian Cancer Drug Resistance: Role of TRAP1 in Oxidative Metabolism-Driven Inflammation. Adv Protein Chem Struct Biol 2017; 108, 163-198.

116.   Vartholomaiou E, Madon-Simon M, Hagmann S, Muhlebach G, Wurst W, Floss T, Picard D. Cytosolic Hsp90alpha and its mitochondrial isoform Trap1 are differentially required in a breast cancer model. Oncotarget 2017; 8, 17428-17442.

117.   Maddalena F, Simeon V, Vita G, Bochicchio A, Possidente L, Sisinni L, Lettini G, Condelli V, Matassa DS, Li Bergolis V, Fersini A, Romito S, Aieta M, Ambrosi A, Esposito F, Landriscina M. TRAP1 protein signature predicts outcome in human metastatic colorectal carcinoma. Oncotarget 2017; 8, 21229-21240.

118.   Coller HA, Grandori C, Tamayo P, Colbert T, Lander ES, Eisenman RN, Golub TR. Expression analysis with oligonucleotide microarrays reveals that MYC regulates genes involved in growth, cell cycle, signaling, and adhesion. Proc Natl Acad Sci U S A 2000; 97, 3260-3265.

119.   Chisholm KM, Bangs CD, Bacchi CE, Molina-Kirsch H, Cherry A, Natkunam Y. Expression profiles of MYC protein and MYC gene rearrangement in lymphomas. Am J Surg Pathol 2015; 39, 294-303.

120.   Caro P, Kishan AU, Norberg E, Stanley IA, Chapuy B, Ficarro SB, Polak K, Tondera D, Gounarides J, Yin H, Zhou F, Green MR, Chen L, Monti S, Marto JA, Shipp MA, Danial NN. Metabolic signatures uncover distinct targets in molecular subsets of diffuse large B cell lymphoma. Cancer Cell 2012; 22, 547-560.